

Author's Response to Reviewer 1

We would like to thank the anonymous reviewer for his or her constructive comments. In this response we provide an answer to all the comments and the indicated changes will be applied in the revised manuscript.

Comment 1: "I was not fully convinced by the vertical discretization approach that the emulator used. First of all, different soil layers have totally different biogeophysical and biogeochemical features. Different layers are experiencing different amount of fresh carbon input (e.g., from fine roots exudates, fine root litter), different microbial community (e.g., fungi/bacteria with different carbon use efficiency), and have different soil structure (e.g., microaggregate, macroaggregate).

Secondly, even the idea of summarizing the above-mentioned vertical difference into one single factor (re) is believable, the value of re should be carefully inferred for this model, rather than taking from other studies.

Thirdly, and most importantly, the vertical discretization, artificially, increase total global SOC stock by 44%. This type of artifact should be removed. My suggestion is that, since ORCHIDEE has one single soil layer, k_0 of ORCHIDEE is supposed to represent the mean turnover rate of the whole soil column. Therefore, the k_0 (equation 5) in the emulator (here aims to represent top soil turnover) should not be k_0 from ORCHIDEE. One approach is to change k_0 in emulator to offset the total SOC stock artifact until it's removed."

Answer: We understand the reviewer's concern regarding the vertical discretization scheme of the emulator and agree that discretizing the SOC over depth is a complex process that has a large impact on the overall SOC stocks. Vertical discretization of SOC has just recently started to be implemented in land surface models. ORCHIDEE is one of the first global land surface models where recently a vertical SOC scheme has been implemented that includes biological production and consumption of SOC, adsorption and desorption processes and diffusion or vertical mixing (Camino-Serrano et al., 2018; Guimberteau et al. 2018). However, for our study we used a simpler version of the ORCHIDEE model without an explicit vertical SOC discretization scheme. One of the main reasons is the need to balance the complexity of the emulator with the computational speed, meaning that including processes such as diffusion would make the

emulator with the carbon balance of each layer more complex and slower, complicating the performance of our erosion simulations. One of the primary reasons for using the C emulator was for its speed and simplicity, so that we could clearly separate and quantify the various effects of soil erosion on the SOC stocks.

However, a vertical SOC profile is necessary to account for smaller SOC erosion rates over time due to the generally decreasing SOC concentration with depth on eroding hillslopes (Hoffmann et al., 2013). Without a vertical SOC profile the removal of SOC by erosion would be most likely overestimated.

To simulate the generally declining SOC with depth (on hillslopes) using the emulator, we let the C input to the soil by belowground litter (roots, shoots) decrease exponentially with depth according to the root-profile exponent ' r ' (equations 6 and 8b of the original manuscript), and we let the soil respiration rate also decrease exponentially with depth using the exponent ' re '. To stay consistent, we use the same values for the exponent ' r ' as in the ORCHIDEE model and make sure that the sum of the belowground litter input to each soil layer is equal to the overall belowground litter input to the soil as simulated by ORCHIDEE. Note that vertical injection of litter from roots in the more sophisticated versions of ORCHIDEE cited above also uses the same root-profile factor ' r '. However, as the ORCHIDEE model version we used has no vertical soil profile, the values for the exponent ' re ' have to be determined either from literature or calibrated in such a way that the vertical discretization does not influence the total SOC respiration and thus the total SOC stock as simulated by ORCHIDEE.

In the original manuscript we used a constant global value for the exponent ' re ' derived from a few local studies in a Belgian landscape. At the same time we assumed that the C pool-dependent soil respiration rate of the original ORCHIDEE model is equal to the surface soil respiration rate ' k_{oi} ' of the vertical C profile in the emulator (equation 5 of original manuscript). This setup resulted in a much higher SOC stock simulated by the emulator with vertical soil profile than simulated by the original ORCHIDEE model. We agree with the reviewer that this artifact should be removed, as it may intervene with the separation and quantification of the effects by soil erosion on the global SOC stock. By deriving ' k_{oi} ' based on the assumption that the average soil respiration rate over the 2m soil profile is equal to the soil respiration rate of ORCHIDEE per grid cell did not result in similar SOC stocks between the emulator and

ORCHIDEE in the case of no soil erosion and no land use change (LUC). Actually, it was rarely possible to find a realistic value for ' k_{oi} ' per grid cell under a constant global ' re ' such that the SOC stocks of the emulator would be similar to those of ORCHIDEE (no soil erosion and no LUC).

Therefore, we decided to calibrate both the exponent ' re ' and variable ' k_{oi} ' for each grid cell and PFT under equilibrium conditions. For this calibration we needed information on the ratios between the SOC stocks of the active, slow and passive pools throughout the soil profile. The old vertical discretization scheme resulted in different ratios between the SOC stocks of the three pools with depth. However, there is very little information or data to constrain the pool ratios globally, mainly because the three SOC pools cannot be directly related to measurements (Elliott et al., 1996). Furthermore, neither the emulator nor the ORCHIDEE model we used include soil processes that may affect these pool ratios with depth, such as vertical mixing by soil organisms, diffusion, changes in soil texture (SOC protection and stabilization by clay particles), limitations by oxygen and by access to deep organic matter by microbes. There is also a lot of discussion on how sensitive SOC is to these other processes. For example, the study of Huang et al. (in revision for the journal *Advances in Modeling Earth Systems*) who implemented a matrix-based approach to assess the sensitivity of SOC showed that equilibrium SOC stocks are more sensitive to input than to mixing for soils in the temperate and high-latitude regions. For all the above-mentioned reasons and to decrease the uncertainty we made the assumption that the ratios between the SOC stocks of the active, slow and passive pools are equal throughout the soil profile in the new vertical soil discretization scheme and similar to the pool ratios derived from ORCHIDEE.

For the transient period (1850-2005), we made ' re ' remain equal to the equilibrium state values, while ' k_{io} ' was derived at a daily time-step to keep to SOC stocks of the emulator similar to those of ORCHIDEE and preserve the yearly variability in the soil respiration rates due to changes in soil climate (no soil erosion and no LUC). Details of how we calibrated the exponent ' re ' and variable ' k_{oi} ' we describe in the section below.

Method for calibration of ' re ' and ' k_{oi} '

We start off by selecting a default value for ' re ' of 2.5 (average between 0 and 5) and then proceed with deriving the values of ' k_{oi} ' according to equations 1-4 described in the following paragraph. After the derivation of ' k_{oi} ' we test if the total SOC stock per grid cell and PFT is

similar to that of ORCHIDEE (difference should be smaller than 1 g m^{-2}). If this is not the case we increase or decrease the value of 're', but make sure that it stays within the range of 0 and 5. If these is no optimized solution for both 're' and 'koi', we use the values that produce the smallest difference in SOC stocks between emulator and ORCHIDEE.

After selecting a value for 're' for a certain grid cell and PFT we first calculated the respiration rate of the surface soil layer (k_0) when all SOC pools are in an equilibrium state, with the following equation:

$$SOC_{orchidee} = \sum_{z=0}^{z=n} \frac{L(z)}{k_0 * e^{-re * z}} \quad (1)$$

Where, $SOC_{orchidee}$ is the total equilibrium SOC stock derived from ORCHIDEE for a certain grid cell and PFT. $L(z)$ is the total litter input to the soil for a certain soil layer discretized according to the root profile.

Then we derived the equilibrium SOC stocks per soil layer as:

$$SOC(z) = \frac{L(z)}{k_0 * e^{-re * z}} \quad (2)$$

Assuming that the ratios between the active, slow and passive SOC pools do not change with depth and are equal to the ratios derived from ORCHIDEE, we can calculate the SOC stocks of each pool with the following equation:

$$1 + \frac{soil_s(z)}{soil_a(z)} + \frac{soil_p(z)}{soil_a(z)} = \frac{SOC(z)}{soil_a(z)} \quad (3)$$

Where, $soil_a(z)$, $soil_s(z)$, $soil_p(z)$ are the emulator derived active, slow and passive SOC stock per soil layer, grid cell and PFT. Now, for the equilibrium state the input is equal to the output, so we can derive k_{0a} , k_{0s} and k_{0p} from the following equations:

$$\sum_{z=0}^{z=n} \left(\frac{L_a(z) + k_{sa} * soil_s(z) + k_{pa} * soil_p(z)}{k_{0a} * e^{-re * z} + k_{as} + k_{ap}} \right) = SOC_a \quad (4a)$$

$$\sum_{z=0}^{z=n} \left(\frac{L_s(z) + k_{as} * soil_a(z)}{k_{0s} * e^{-re * z} + k_{sa} + k_{sp}} \right) = SOC_s \quad (4b)$$

$$\sum_{z=0}^{z=n} \left(\frac{k_{sp} * soil_s(z) + k_{ap} * soil_a(z)}{k_{0p} * e^{-re * z} + k_{pa}} \right) = SOC_p \quad (4c)$$

Where, L_a is the total litter input to the active SOC pool, L_s is the total litter input to the slow SOC pool. SOC_a , SOC_s , SOC_p are the total active, slow and passive SOC per grid cell and PFT, respectively, derived from ORCHIDEE. k_{as} , k_{ap} , k_{sa} , k_{sp} , k_{pa} are the coefficients determining the fluxes between the SOC pools.

In the transient period (no land use change or erosion) we assume a time-constant ' re ' fixed to the equilibrium state. Using the mass-balance approach we can find the daily values for k_{0a} , k_{0s} , k_{0p} per grid cell and PFT with:

$$\frac{dSOC_a}{dt} = \sum_{z=0}^n (L_a(z, t) + k_{sa} * soil_s(z, t - 1) + k_{pa} * soil_p(z, t - 1) - (k_{0a}(t) * e^{-re*z} + k_{as} + k_{ap}) * soil_a(z, t - 1)) \quad (8a)$$

$$\frac{dSOC_s}{dt} = \sum_{z=0}^n (L_s(z, t) + k_{as} * soil_a(z, t - 1) - (k_{0s}(t) * e^{-re*z} + k_{sa} + k_{sp}) * soil_s(z, t - 1)) \quad (8b)$$

$$\frac{dSOC_p}{dt} = \sum_{z=0}^n (k_{sp} * soil_s(z, t - 1) + k_{ap} * soil_a(z, t - 1) - (k_{0p}(t) * e^{-re*z} + k_{pa}) * soil_p(z, t - 1)) \quad (8c)$$

In case there was no solution for the ' k_{0i} ' at a certain time-step we took the values from the previous time-step.

Implications of the new vertical discretization scheme

After implementing the above-mentioned empirical adjustments to the vertical SOC discretization scheme of the emulator, we found that the resulting SOC stocks for the equilibrium state are close to those of ORCHIDEE with some small deviations (Fig. S1). It was not always possible to precisely match the SOC stocks of the emulator and ORCHIDEE and at the same time have realistic vertical SOC profiles, where the ' re ' variable varies between 0 and 5.

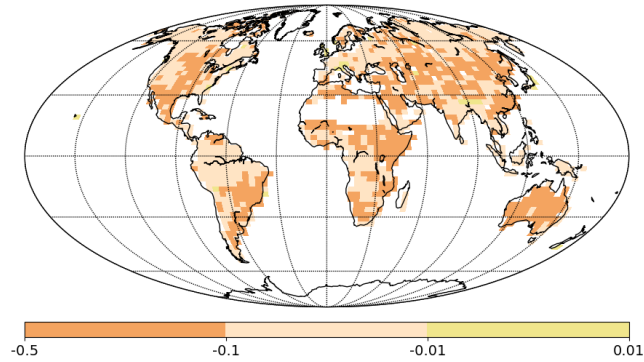


Figure S1: The difference in SOC stocks between the emulator and ORCHIDEE as a ratio (%) of the ORCHIDEE SOC stocks for the equilibrium state of the year 1850 without soil erosion. Positive values indicate larger SOC stocks of the emulator compared to the ORCHIDEE model, and negative values indicate smaller SOC stocks of the emulator compared to the ORCHIDEE model.

PFT number	PFT description	Area-weighted mean re
0	Bare soil	2.5
1	Tropical broad-leaved evergreen	0.72
2	tropical broad-leaved raingreen	1.33
3	temperate needleleaf evergreen	1.29
4	temperate broad-leaved evergreen	1.25
5	Temperate broad-leaved summergreen	1.09
6	boreal needleleaf evergreen	1.33
7	boreal broad-leaved summergreen	1.13
8	boreal needleleaf summergreen	0.93
9	C3 grass	2.03
10	C4 grass	2.3
11	C3 agriculture	0.73
12	C4 agriculture	0.78

Table S1: Global area-weighted average ' re ' values per PFT

Figure S2 shows that also for the transient period of simulation S4 (no erosion or LUC) the total SOC stocks are similar between emulator and the ORCHIDEE model. The difference between the SOC stock of the emulator and ORCHIDEE are between -1 and 0% of ORCHIDEE SOC

stocks for most grid cells, however, the maximum difference can reach -10% for some grid cells. The total global SOC stock of the emulator in the year 2005 deviates by -0.5% from the SOC stock of ORCHIDEE. This differences between the emulator and ORCHIDEE are due to the fact that there was not always an optimal and realistic solution for ' k_{0i} ' and ' re '.

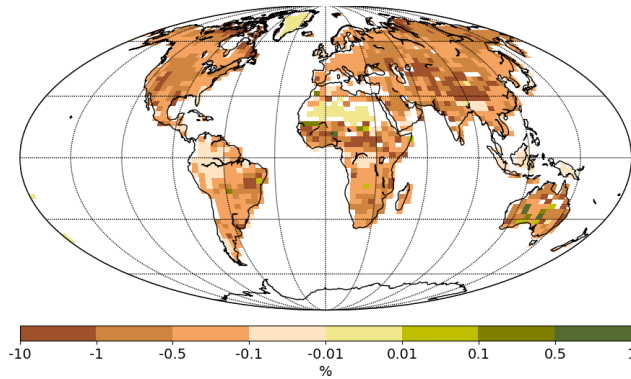


Figure S2: The difference in SOC stocks between the emulator and ORCHIDEE as a ratio (%) of the ORCHIDEE SOC stocks averaged over the period 1996-2005 for simulation S4 (no erosion, no LUC). The total Positive values indicate larger SOC stocks of the emulator compared to the ORCHIDEE model, and negative values indicate smaller SOC stocks of the emulator compared to the ORCHIDEE model.

Although the new vertical discretization scheme did change the values of the SOC stocks and the related changes to the SOC stocks during the transient period, the main trends and findings of this study remain the same. In the following paragraph we describe the changes to our results, figures and tables as will be presented in the revised manuscript.

Changes in the manuscript: We included the above-mentioned derivation of the variables of the new vertical discretization scheme of the emulator and the argumentation behind it, as explained above, in the revised manuscript in chapter 2.3. We include table S1 with the global mean values for the ' re ' exponent per PFT in the supplementary material.

We also changed the tables 2 to 7 of the original manuscript, where we include the new values for changes in SOC stocks and SOC erosion rates. Furthermore, we adapted figures 4B,4D,4F,4H, 5C,5D,5E,6A,7,8A,8B,8C and 9 according to the new results of the simulations with the new vertical discretization scheme. The main changes to the results in the abstract,

chapter 3, 4 and 5 of the manuscript are provided below. The uncertainty ranges provided in the results are related to comment 12 of reviewer 2.

We make the following changes to the abstract:

L27: “We found that over the period 1850-2005 AD acceleration of soil erosion leads to a total potential SOC removal flux of 74 ± 18 Pg C of which 79-85% occurs on agricultural, pasture and natural grass lands”

L29: “Including soil erosion in the SOC-dynamics scheme results in an increase of 62% of the cumulative loss of SOC...”

L31:” This additional erosional loss decreases the cumulative global carbon sink on land by 2 Pg for this specific period,...”

We make the following changes in the results chapter:

L417: “This global soil loss flux (here ‘loss’ meaning horizontal removal by erosion) leads to a total SOC loss flux of 0.52 ± 0.14 Pg C y^{-1} of which 26 to 33% are attributed to agricultural land and 54 to 64% to grassland (CTR, Fig 4)”

L421: “The total soil and SOC losses in the year 2005 are an increase of 11-19% and 23-35%, respectively, compared to 1850”

L429: ” We found that the total soil erosion flux on agricultural land increased with 55-58% by the year 2005 compared to 1850, while the SOC erosion flux increased with 11-70% (Fig. 4) and led to a cumulative SOC removal of 22 ± 5 Pg.”

L431” On pasture land and grassland, the soil erosion flux increased only with 8-20%, while the SOC erosion flux increased with 44-54% (Fig. 4) and led to a cumulative SOC mobilization of 38 ± 7 Pg since 1850.”

L442: ” In total 7183 ± 1662 Pg of soil and 74 ± 18 Pg of SOC is mobilized across all PFTs by erosion during the period 1850 - 2005, which is equal to approximately 46-74% of the total net flux of carbon lost as CO₂ to the atmosphere due to LUC...”

L462:” We calculated a total global SOC stock for 2005 in the absence of soil erosion (S3) of 1284 Pg, which is a factor of 0.73 lower than the total SOC stock from GSCE (Shangguan *et al.*, 2014) for a soil depth of 2m (Table 5).”

L466:” Including soil erosion (S1) leads to a total SOC stock of 1001 ± 58 Pg for the year 2005 (Table 5). We also find that including soil erosion in the SOC-dynamics scheme slightly improves the root mean square error (RMSE) between the simulated SOC stocks and those from GSDE, for the top 30cm of the soil profile. This improvement in the RMSE occurs especially in highly erosive areas.”

L486:” This flux is paralleled by a SOC loss flux of 0.16 ± 0.06 Pg C y⁻¹ after including soil erosion in the CTR simulation (Fig. 4).”

L495:” Furthermore, we find a cumulative soil loss of 1888 ± 753 Pg and cumulative SOC removal flux of 22 ± 5 Pg from agricultural land over the entire time period (CTR simulation). “

We make the following changes in the discussion chapter:

L507: “...When considering our best estimated soil erosion rates and assuming that the SOC mobilized by soil erosion in the CTR simulation is all respired, we find an overall global SOC stock decrease that is 62 % larger compared to a world without soil erosion...”

L582:” We find that the global SOC stock decreases by 17 Pg due to LUC only during 1850 – 2005 (Fig. 6A, S3-S4). The overall change in carbon over this period summed up over all biomass, litter, SOC, and wood-product pools due to LUC without erosion is a loss of 102 Pg C which lies in the range of cumulative carbon emissions by LUC from estimates of previous studies (Houghton and Nassikas, 2017; Li et al., 2017; Piao et al., 2009)”

L585: “When we use our best estimated soil erosion rates in the SOC-dynamics scheme of the emulator we find that the LUC effect on the global SOC stock is amplified by 4Pg or a factor of 1.2 (S1-S2, Fig. 6A)”

L591: “This leads to a total change in the overall carbon stock on land of -106 Pg.”

L610: ” ...and leads even to a net cumulative sink of carbon on land over this period of about 30 Pg C (S3)”

L613:” In the presence of soil erosion, climate variability and the atmospheric CO₂ increase lead to a slightly smaller net cumulative sink of carbon over land of 28 Pg C (S1)...”

We make the following changes to the conclusion chapter:

L713: “This potential soil loss flux mobilized 74 ± 18 Pg of SOC across all PFTs, which compares to 60% of the total net flux of carbon lost as CO₂”

L715:” When assuming that all this SOC mobilized is respired we find that the overall SOC change over the period 1850-2005 would increase by 62% and reduce the land carbon sink by 2 Pg.”

Figure 4: There are no significant changes in the historical trends due to the new vertical discretization scheme, except for the overall values.

Figure 5: Only slight changes in the spatial variability of the SOC stocks and SOC erosion rates are observed, which are due to the new vertical discretization scheme.

Figure 6A: No significant changes in the temporal trends of the cumulative SOC stock are observed when the new vertical discretization scheme is used. However, the overall changes in the cumulative stocks are smaller.

Figure 7: The cumulative SOC stock change in the original manuscript was wrongly projected and is corrected here. The grassland SOC stocks should decrease instead of increase. Overall, the historical trends in the cumulative SOC stocks follow closely the changes in the respective vegetation fractions. The overall changes in SOC stocks are smaller here compared to the figure in the original manuscript due to the new vertical scheme.

Figure 8: no significant changes are observed in the plots due to the new vertical scheme.

Figure 9: Some slight changes are observed in the plot due to the new vertical scheme.

Comment 2: “Land use change map. The LUC is prescribed by PFT fractional change derived from Peng 2017. Wondered how this LUC dataset differs from Land-Use Harmonization (LUH2), the new CMIP6 land use change dataset. Given that LUC is a dominant factor of SOC erosion, I am curious about the uncertainty of SOC erosion, induced by using different LUC estimate (e.g., Peng 2017 vs LUH2).”

Answer: The PFT fractional map is based on LUHv2 land use dataset, historical forest area data from Houghton (for large regions) and present day forest area from ESA CCI satellite land cover data (Peng et al., 2017). The historical forest data from Houghton and the latest satellite land cover data from ESA are the best estimates that currently exist on forest area. Figure S3 shows

that if the forest is not constrained with methods described by Peng et al. (2017), there is a stronger decrease in forest area over the period 1850-2005. Also the grassland shows an increasing trend, while in the PFT map with constrained forest the grassland shows globally a slight decreasing trend. In the rest of the text we will refer to the PFT map constrained with data on forest area as the ‘constrained PFT map’ and to the other PFT map as the ‘unconstrained PFT map’.

We agree with the reviewer that different land use data can result in large uncertainties in both SOC stocks and soil erosion rates. To show the potential uncertainty in our results due to uncertainties in underlying land use data we performed 4 additional simulations (S1 to S4) using the unconstrained PFT map and the new vertical discretization scheme.

Differences in global average soil erosion rates between the different PFT maps are small (Fig. S4), mainly because the C-factor of our Adjusted RUSLE model is similar for forest and dense natural grass. As the change in cropland area globally was not very different between the 2 PFT maps, the overall soil erosion rates were similar. We expect, however, that the changes in soil erosion rates between the 2 PFT maps can be significant in areas where the change in forest area was significant over the historical period.

In contrast to the soil erosion rates, the 2 PFT maps resulted in significant differences in the SOC erosion rates and cumulative changes in SOC stocks during the transient period (Fig. S4). The global SOC stock in the equilibrium state without soil erosion (S3) is 8 % higher when the unconstrained PFT map is used, due to a larger global forest area in this map at 1850. The higher global SOC stock of the PFT map without constrained forest area lead to higher SOC erosion rates (Fig. S4b). According to the unconstrained PFT map, soil erosion leads to a total SOC removal of 79 Pg (S1) over the period 1850-2005, which is 6Pg larger than the total SOC removal by soil erosion under the constrained PFT map.

Interestingly, according to the unconstrained PFT map, the global cumulative SOC stock change over 1850-2005 under soil erosion and LUC (S1) is 60% smaller than the stock derived using the constrained PFT map. This is most likely due to the higher forest area at the start of the period 1850-2005, leading to a larger increase in SOC stocks by increasing atmospheric CO₂ concentrations. The global LUC effect on the SOC stocks of both PFT maps is found to be similar (Fig 5C, D).

Figure S3: Changes (%) in forest (green), grass (light-green) and crop (red) fractions over the period 1850-2005 with respect to the year 1850AD. The dashed lines represent data from the PFT map without constrained forest, while the straight lines represent data from the PFT map from Peng et al. (2017).

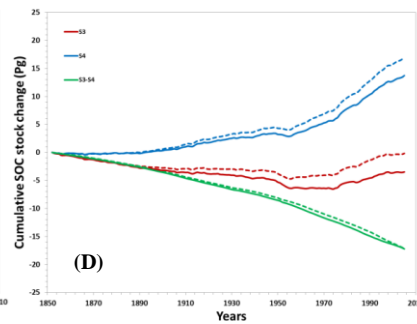
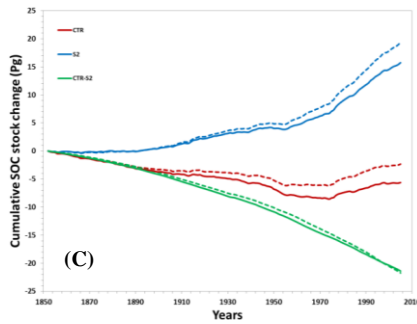
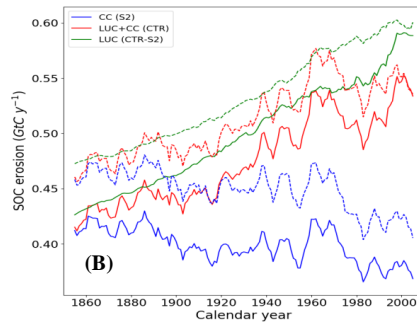
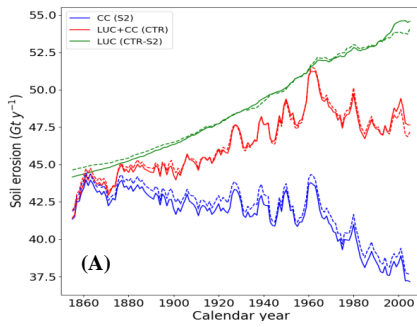
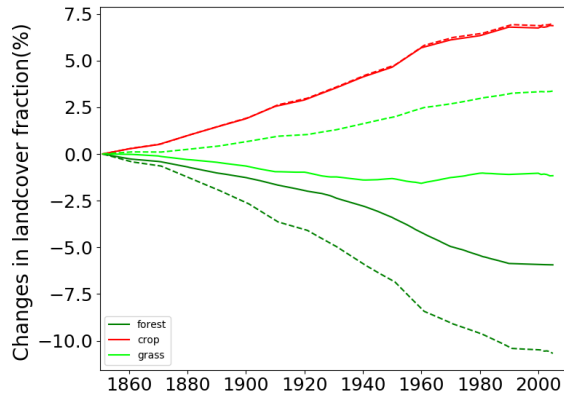


Figure S4: Differences in (A) soil and (B) SOC erosion rates and (C and D) cumulative SOC stock changes between the PFT map that is constrained by forest area data (straight lines) and the PFT map that is not constrained by forest area data (dashed lines).

Changes in the manuscript:

The uncertainty due to different land use maps, as discussed above, will be discussed in chapter 4.4 of the manuscript, and we will mention the above-mentioned changes to the erosion rates and SOC stocks. The new figures S3 and S4 will be included in the supplementary material.

Specific comment 1: “L16: The first sentence gives me an incorrect hint that the paper is going to talk about agriculture activity accelerates soil erosion”

Answer: We agree that this may be misleading and changed this sentence to: “Erosion is an Earth System process that transports carbon laterally across the land surface, and is currently accelerated by anthropogenic activities. Anthropogenic land cover change has accelerated soil erosion rates by rainfall and runoff substantially, mobilizing vast quantities of soil organic carbon (SOC) globally.”

Specific comment 2: “L43: 1.0 Pg, does it include fire emission?”

Answer: yes it does

Specific comment 3: “L61 what is bookkeeping models?”

Answer: Bookkeeping models are methods/tools to calculate land use change emissions by keeping track of the carbon stored in different pools before and after land use changes take place. These methods also keep track of the CO₂ emitted after land use change has taken place.

Specific comment 5: “L337 What’s the meaning of randomly projected? A more reasonable way is to repeat 1990-1910 climates during 1850-1900.”

Answer: “Randomly projected”, means that the climate of the years after 1900 was randomly assigned to the years between 1850 and 1900 because the climate data of CRU-NCEP was only available starting from year 1900. If we would choose to repeat the climates of 1900-1910, we would risk including the effects of extreme climate conditions multiple times.

Changes in the manuscript:

In L337 we will add: “The random projection of the climate data is necessary to avoid the risk of including the effects of extreme climate conditions multiple times when only a certain decade is used repeatedly.”

Specific comment 6: “L556 “Also, intense soil erosion is typically found in mountainous areas where climate variability has significant impacts, while at the same time these regions are usually poor in SOC.” It’s not clear in the manuscript whether or not ORCHIDEE has topography information? In another word, if ORCHIDEE simulates a low SOC stock over the grid cells that have mountains, is that because of the topographical feature of this gridcell can not hold a lot of SOC in ORCHIDEE? Or because of other reasons such as climate constraints (e.g., colder in mountain area)?”

Answer: ORCHIDEE has no soil depth information and thus cannot simulate low SOC stocks due to the fact that the gridcell cannot hold a lot of SOC. Low SOC might however be a result of the plant productivity, the climate (temperature and precipitation), soil moisture and clay content (which is a constant variable). ORCHIDEE has, however, topographical information such as slope that determines the flow directions for water/runoff and affects hydrological parameters such as soil moisture content.

Changes in the manuscript: L556: “Also, intense soil erosion is typically found in mountainous areas where climate variability has significant impacts, while at the same time these regions are usually poor in SOC due to unfavorable environmental conditions for plant productivity.”

Specific comment 7: “L577 CO₂ fertilization effects on NPP is not fully convincing here, because ORCHIDEE does not have nutrient constraints. OCN might be a better surrogate model to be able to say something about CO₂ fertilization effect on NPP.”

Answer: In the ORCHIDEE model version we used the nutrients are indeed absent. Our intention, however, was to show the complete picture of possible direct and indirect interactions of soil erosion with the C cycle with the current model setup. The representation of nutrients in global land surface models is new and the related uncertainties are not well quantified. We work with a more or less simple version of ORCHIDEE and the C emulator to be able to understand and quantify the effects of soil erosion on the C cycle.

Changes in the manuscript:

L636: “Finally, it should be mentioned here that the absence of nutrients in the current version of the ORCHIDEE model may result in an overestimation of the CO₂ fertilization effect on NPP and may introduce biases in the effect of erosion on SOC stocks under increasing atmospheric CO₂ concentrations. Soil erosion may also lead to significant losses of nutrients, especially in agricultural areas. For a more complete quantification of the effects of soil erosion on the carbon cycle, nutrients have to be included in future studies.”

Specific comment 8: ” Figure 4. I do not fully understand why climate change either decrease or not change erosion?

Answer: With climate change we mean temperature and precipitation changes. For soil erosion only precipitation changes are of interest. Globally we find that average yearly precipitation shows a slightly decreasing trend over the period 1950 – 2005 according to the ISIMIP2b dataset used to calculate soil erosion rates. A global smaller total precipitation with respect to 1850 AD will lead to smaller soil erosion rates when LUC is not included. The decrease in total precipitation over land is mostly coming from the tropics, where due to large precipitation amounts a change in precipitation can alter soil erosion significantly. At the same time precipitation is very variable and might not lead to a significant global net change in soil erosion rates over the total period 1850-2005. This result might be contradictory to the fact that major soil erosion events are caused by storms. But in our case we model only rill and interrill erosion, which is usually a slow process and previous studies have shown that land use change is usually the main driver of behind accelerated rates of this type of soil erosion. Furthermore, there are very few studies that have quantified the individual effects of precipitation change versus land use change on soil erosion rates over a sufficiently long time period. Therefore, it is difficult to verify this result. However, our soil erosion model performs well for present-day and therefore any possible biases here could be mainly related to biases in precipitation rates, and soil parameters. We agree that this is an interesting point raised by the reviewer and added some additional sentences explaining the trend in the beginning of chapter 4.2.

Changes in the manuscript:

L536: “The global decrease in precipitation in many regions worldwide, especially in the Amazon, as simulated by ISIMIP2b, lead to a slight decrease in soil and SOC erosion rates (Fig.

4). At the same time precipitation is very variable and might not lead to a significant global net change in soil erosion rates over the total period 1850-2005. This result might be contradictory to the fact that major soil erosion events are caused by storms. But in this study we only simulate rill and interrill erosion, which are usually slow processes. In addition, previous studies have shown that land use change is usually the main driver behind accelerated rates of these types of soil erosion. Our study confirms this observation.”

Author’s Response to Reviewer 2

We would like to thank the anonymous reviewer for his or her constructive comments. In this response we provide an answer to all the comments and the indicated changes will be applied in the revised manuscript.

Comment 1: “The emulator used in this study seems to have various limitations that make the numbers presented quite uncertain – further discussion on, and quantification of, these uncertainties is warranted and would greatly improve this manuscript. Specifically, I would have liked to see additional support for the SOC model formulation, parameters, and built-in feedbacks chosen for the emulator, as well as support for its vertical discretization and parameterization.

The carbon emulator is supposed to describe the carbon pools and fluxes exactly as in ORCHIDEE, yet the total global SOC stocks from the emulator are 44% higher than that of the original ORCHIDEE model. This is a big difference. What does this tell us about the accuracy and applicability of the emulator, and how do the SOC stocks of the two models compare to the Harmonized World Soil Database (HWSD) and other global SOC databases? Additional major comments/questions, especially those regarding the assumptions and methods used, are detailed below.”

Answer: We modified the vertical discretization scheme of the emulator in such a way that the total SOC stock of each grid cell, PFT and C pool is close to that of ORCHIDEE when soil erosion and land use change is deactivated (0.5% max difference in total global SOC stock). For this we calibrated both the exponent ‘ re ’ and variable ‘ k_{oi} ’ of equation 8 in the manuscript for each grid cell and PFT under equilibrium conditions, such that the total soil respiration per grid cell, PFT, and soil C pool of the emulator would be similar to that of the ORCHIDEE model. For the transient period (1850-2005), we made ‘ re ’ remain equal to the equilibrium state values,

while values for ' k_{i0} ' were derived at a daily time-step to keep to SOC stocks of the emulator similar to those of ORCHIDEE and preserve the yearly variability in the soil respiration rates due to changes in soil climate (soil erosion and land use change were deactivated). Details of how we calibrated the exponent ' re ' and variable ' k_{oi} ' we describe in our response to Reviewer 1 and in the manuscript after line 274. The modified vertical discretization scheme did change the values of the SOC stocks and SOC removal rates, because with this scheme we simulated total SOC such as in the ORCHIDEE model without soil erosion and land use change. However, the overall trends in soil and SOC erosion rates and cumulative changes in SOC stocks during the transient period did not change significantly and the main findings of our study remain unchanged. For more details on the changes in our manuscript related to the modified vertical discretization scheme see our detailed response to reviewer 1.

We performed a comparison of our simulated SOC stocks to the Global Soil Database for Earth System Modeling (GSDE), as is described in paragraph 3.2 and the new table 5 of the manuscript (with results based on the new vertical discretization scheme). However, we abstained from a more in-depth comparison as our emulator and ORCHIDEE do not include various soil processes that have been proven to affect SOC substantially such as vertical mixing, diffusion, priming, changes in soil texture, C rich organic soils formation, etc.

It should be noted that there are also large uncertainties in the global soil databases (Hengl et al., 2014; Scharlemann et al., 2014; Tifafi et al., 2018), which makes the exact quantification of the uncertainties of the resulting SOC dynamics simulated by our emulator difficult.

After applying the modifications to the vertical SOC discretization scheme, we performed a simulation with soil erosion and land use change activated (S1) and compared the resulting SOC stocks with those from the GSDE. Figure S1 shows that our emulator, and the ORCHIDEE model in general, underestimates SOC stocks globally, except for the high-latitudes.

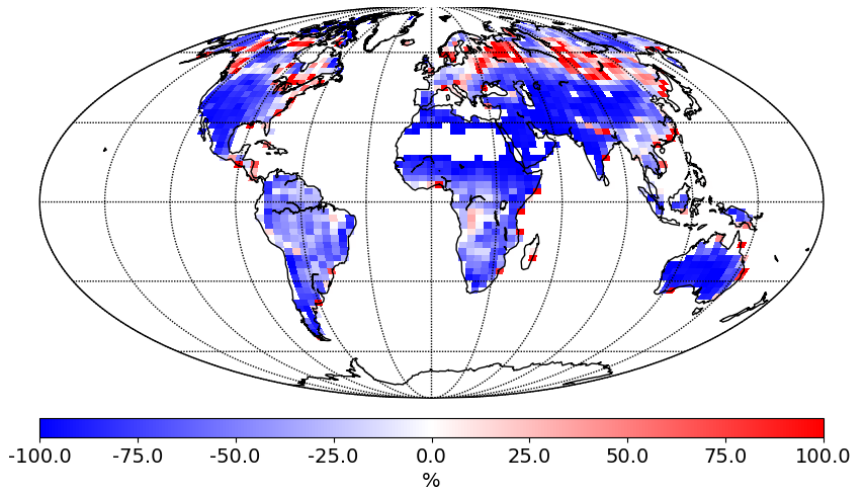


Figure S1: Difference between SOC stocks of the emulator (simulation S1) and the SOC stocks of GSDE as a percentage of the SOC stocks of GSDE till 2m depth. Red colors show larger SOC stocks by the emulator, while blue colors indicate smaller SOC stocks by the emulator compared to GSDE.

Changes in manuscript: We put figure S1 in the supplementary material. Furthermore, the values of table 5 of the manuscript are updated and presented in the revised manuscript.

L493:” We did not perform a more in-depth comparison as our emulator and ORCHIDEE do not include various soil processes that have been proven to affect SOC substantially such as vertical mixing, diffusion, priming, changes in soil texture, carbon rich organic soils formation, etc. The ORCHIDEE model we use also lacks processes such as nitrogen and phosphorus limitations and priming, which affect the productivity and SOC decomposition (Goll *et al.*, 2017; Guenet *et al.*, 2016). The emulator also misses the SOC transport and deposition after erosion, and there is a general uncertainty in the simulation of underlying processes that govern the SOC dynamics (Todd-Brown *et al.*, 2014). Finally, large uncertainties in the global soil databases (Hengl *et al.*, 2014; Scharlemann *et al.*, 2014; Tifafi *et al.*, 2018), complicate the exact quantification of the uncertainties of the resulting SOC dynamics simulated by our emulator.”

Specific comment 1: “L143: What are the limitations of not including these processes in the emulator? Can it capture all feedbacks and dynamics?”

Answer: Some of these processes are already included in the ORCHIDEE model, which is the basis for the C emulator but other feedbacks on SOC are missing in the original ORCHIDEE model such as the effect of SOC on the hydrology or on the thermic of the model. Nevertheless, our main objective here was to present a tool able to evaluate erosion fluxes at global scale using a ‘state-of-art’ land surface model outputs and estimate the drivers of erosion at global scale. In addition, this study did not focus on the feedbacks of soil erosion and land use change on NPP, the hydrological cycle or nutrient cycle and therefore it was decided not to incorporate soil erosion processes directly into ORCHIDEE, but rather use the C emulator concept instead. Not including these processes explicitly in the emulator does not change the simulated SOC dynamics in our study. However, the emulator has a flexible structure and could be made more complex depending on the needs, such as including a more sophisticated vertical discretization scheme.

The main idea of the emulator was to use a modeling tool that does not require much computational power but that still incorporates the basic processes and variables for simulating large-scale SOC dynamics under soil erosion and land use change. Many simulations were needed to quantify the various effects of soil erosion on the C cycle and to calibrate the model parameters. The C emulator was in this case a convenient tool, as it is fast and its structure allows to easy switch processes on or off.

Changes in manuscript: See our answer to the next comment.

Section 2.1 L158: “Our main objective here is to present a tool able to evaluate erosion fluxes at global scale using a ‘state-of-art’ land surface model outputs and estimate the drivers of erosion at global scale.”

Specific comment 2: “L142-143: although originally calculated by complex equations, the dynamic evolution of each pool can be described using the first-order model” – why were the complex equations needed initially then? Again, what are the limitations of this first-order model?

Answer: The limitations of this first-order model are the incapability to capture feedbacks on the hydrological processes or on the NPP (see answer to previous comment). However, because the SOC is represented by first order equations inside ORCHIDEE and the complex equations only

compute the modifier to the default coefficients, and as our study focused on the effects of soil erosion on the SOC dynamics, we decided to use the C emulator, assuming that erosion will not significantly impact soil physics (and in turn decomposition) affecting SOC. The complex equations, such as photosynthesis and hydrological processes are needed to simulate realistically the changes in biomass, litter and soil respiration over time, which is done by ORCHIDEE. In the original ORCHIDEE simulations, these processes are explicitly simulated on a 30 min time step. Such a time step is needed for coupled simulations with a climate model, but makes the model CPU intensive, and there is no need for such high-resolution calculations of 'fast' C fluxes for erosion induced effects on SOC. In the emulator, all C fluxes between ecosystem compartments (with and without erosion) are exactly the same as the original ORCHIDEE, assuming that there is no feedbacks between erosion and these fluxes. The C emulator is much more computational efficient than the original ORCHIDEE because it does not require to compute all 'fast' processes for all simulations. The emulator thus allows us to conduct a lot of simulations (e.g. with and without climate change, with and without CO₂ fertilization, with and without land use change, with and without erosion), and at the same time keep the main features (except erosion) of the original ORCHIDEE simulation.

Changes in manuscript: L144: "...Eq.1. Complex equations, such as photosynthesis and hydrological processes are needed to simulate realistically the carbohydrates input to carbon pools and the moisture and temperature conditions controlling litter and soil carbon decomposition over time. All the processes that determine surface and soil temperature and soil moisture, are calculated by the ORCHIDEE LSM on a 30 minute time-step. Such a time-step is needed for coupled simulations with a climate model, but makes the LSM model CPU intensive. However, there is no need for such high temporal resolution calculations of 'fast' carbon and energy fluxes to account for erosion-induced effects on SOC stocks. The addition of erosion is here supposed to impact only carbon pools, and to have no feedbacks on soil moisture, soil temperature and photosynthesis. Therefore, we decided to use the emulator concept rather than incorporating erosion processes directly into ORCHIDEE. For each carbon pool..."

Specific comment 3: “L196: What does the passive pool correspond to (as a measurable pool)? Why is there no transfer from p to s (k_{ps})? Why no input to this pool?”

Answer: The distribution of SOC into an active, slow and passive pool and the transfer rates between these pools are based on the work of Parton et al. (1988). These pools are defined by their different residence times. The active, slow and passive SOC pools have a residence time of 1.5, 25 and 1000 years, respectively. That study defines the passive pool as a pool that is very resistant to decomposition and includes physically and chemically stabilized SOM. The proportions of the decomposition products which enter the passive pool from the slow and active pools increase with increasing soil clay content. Passive C is thus not directly produced from litter input but active or slow C has to be stabilized first to become passive C. Then, the original model of Parton et al., (1987) assumes that when the passive pool is decomposed by microorganisms, they produce metabolites corresponding to more labile materials that are released in the soil solution during microbial death and the associated cell lysis. For these reasons, they considered that the decomposed passive pool can only be recycled into the active pool.

Changes in manuscript: L196: “The SOC pools are based on the study of Parton et al. (1988) and are defined by their residence times. The active SOC pool has the lowest residence time (~1.5 years) and the passive the highest (1000 years).”

Specific comment 4: “L209: Does this allow for emergent differences in the relative distribution of the three pools with depth? (e.g., relatively more passive C than active C with depth, etc.)”

Answer: Yes, the old vertical discretization scheme allowed for different relative distributions of the three pools with depth. However, we changed this aspect by assuming that the ratios between the three pools do not change with depth so that the relative distribution is the same. We made this assumption as we have not enough data to clearly determine how the ratios between the pools change should change with depth (see reply to rev #1). In addition, we do not simulate the

underlying processes that would allow for changing ratios between the SOC pools such as changing clay content with depth, diffusion, bioturbation.

Specific comment 5: “L196 (old manuscript): "The SOC respiration rates for the topsoil layers are equal to those from ORCHIDEE". But how about subsoil respiration? Does the emulator have more respiration overall then? Please clarify how the models compare.”

Answer: We modified the vertical discretization scheme, so that the emulator now has a similar SOC respiration rate as ORCHIDEE without soil erosion or land use change. See our response to the first comment and to the comments of reviewer 1.

Specific comment 6: “L256: "total global SOC stock is approximately 44% larger than that from the original ORCHIDEE model" – what does this tell us about the accuracy and applicability of the emulator? This seems to be a big difference. How do the SOC stocks of the two compare to the HWSD and other global SOC databases?”

Answer: We modified the vertical discretization scheme, where the emulator has similar SOC stocks as ORCHIDEE without soil erosion or land use change. For more details see our response to the first comment of reviewer 1.

Specific comment 7: “L226: How are these fractions determined? What are the implications of the uncertainty in this partitioning?”

Answer: Above and below-ground litter consists out of plant residues and organic animal excreta that are partitioned into structural and metabolic pools as a function of the lignin to N ratio in the residue (Parton et al., 1988). The lignin and N ratios are usually prescribed per PFT and derived from plant-trait databases. This partitioning is prescribed by Parton et al. (1988) and followed by Krinner et al. (2005). The structural litter pool has a slower decay rate and contains the more recalcitrant molecules, while the metabolic pool has a faster decay rate and contains labile plant material. The decay rates are a function of temperature and humidity (Krinner et al., 2005). The lignin fraction of the plant material does not go through the active pool but is

assumed to go directly to the slow C pool as the structural plant material decomposes. This is why part of the decomposed structural litter pool goes to the active SOC pool and another to the slow SOC pool. Metabolic litter can be decomposed into active SOC and could also form a mineral-stabilized SOC (slow SOC pool, Cotrufo et al., 2015). The CENTURY model simulates the dynamics of C and nutrients (Parton et al., 1988), and is widely applied and tested in Land Surface Models. There are definitely large uncertainties in the partitioning of the litter pools, however, it is not in the scope of this paper to discuss these uncertainties.

Changes in manuscript: L230: “These litter fractions are based on the Century model as introduced by Parton et al.(1988) and later implemented inside ORCHIDEE (Krinner et al., 2005).”

Specific comment 8: “L337: Why "randomly projected"? Please explain how and why.”

Answer: “Randomly projected”, means that the climate of the years after 1900 was randomly assigned to the years between 1850 and 1900 because the climate data of CRU-NCEP was only available starting from year 1900. If we would choose to repeat for example the climates of 1900-1910, we would risk including the effects of extreme climate conditions multiple times, which is not the case when a random projection is used.

Specific comment 9: “L359: But you used CRU-NCEP for ORCHIDEE... what are the caveats of using different climate datasets for each model?”

Answer: We compared the historical trend in yearly total precipitation between CRU-NCEP and ISIMIP2b, see figure S2. We find that although the ISIMIP2b shows a higher overall precipitation amount, the temporal trend and variability are similar to that of CRU-NCEP. If we would use CRU-NCEP to calculate the soil erosion rates, we expect that the new soil erosion rates would fall inside the uncertainty range created by calculation of the R- and the C-factors of the Adj. RUSLE (see answer to the last comment).

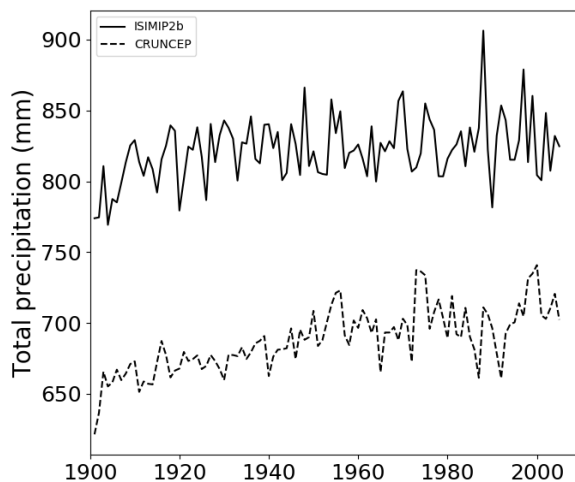


Figure S2: Temporal trend in yearly total, global average precipitation derived from ISIMIP2b (straight line) and CRU-NCEP (dashed line).

Specific comment 10: “L366: Why this dataset? How does it compare to the HWSD and SoilGrids (Hengl et al. PLoS ONE 2014, 2017) datasets?”

Answer: The GSDE is based on the SoilMap of the World (FAO, 1995, 2003) and various regional and national soil databases. It is available at a 1km resolution and at 5 arcmin resolution and contains updated soil information and more soil variables such as nutrients. The GSDE is based on several regional soil maps and is more up to date on soil information than the HWSD but both products compared relatively well since they shared several data (Shangguan et al., 2014). We did not test the SoilGrids data, which is based on a different approach. A recent publication showed that SoilGrids give different results compared to HWSD (Tifafi et al., 2018) but regarding the difference between the products we decided to use only one of them already used to evaluate erosion process and then be more comparable with previous publications (Naipal et al., 2015, 2016).

Specific comment 11: L415: How uncertain are these numbers given the model formulation assumptions, land-use maps, and methods used? It would help to see a sensitivity analysis and some uncertainty ranges.

Answer: We performed 4 additional simulations with a different PFT map, which is also based on the LUH2 land use dataset but where the historical forest area change that is not constrained by data as done by Peng et al. (2017). We used these simulations to show the differences to our results when other land use maps are used. If the forest is not constrained with methods described by Peng et al. (2017), there is a stronger decrease in forest area over the period 1850-2005. Also the grassland shows an increasing trend, while in the PFT map with constrained forest the grassland shows globally a slight decreasing trend. In the rest of the text we will refer to the PFT map constrained with data on forest area as the ‘constrained PFT map’ and to the other PFT map as the ‘unconstrained PFT map’. Differences in global average soil erosion rates between the different PFT maps are small, however, there are significant differences in the SOC erosion rates and cumulative changes in SOC stocks during the transient period. According to the unconstrained PFT map, soil erosion leads to a total SOC removal of 79 Pg (simulation S1 with the new vertical discretization scheme) over the period 1850-2005, which is 6Pg larger than the total SOC removal by soil erosion under the constrained PFT map.

Interestingly, according to the unconstrained PFT map, the global cumulative SOC stock change over 1850-2005 under soil erosion and LUC (S1) is 60% smaller than the stock derived using the constrained PFT map. This is most likely due to the higher forest area at the start of the period 1850-2005, leading to a larger increase in SOC stocks by increasing atmospheric CO₂ concentrations. The global LUC effect on the SOC stocks of both PFT maps is found to be similar. For more details and our changes in the manuscript see our answer to comment 2 of reviewer 1.

Specific comment 12: “L645: (Section 4.4) with all of these model limitations, it would be nice to have a rough quantification of uncertainties.”

Answer: We agree with the reviewer that quantifying the uncertainty is important. Therefore, we derived an uncertainty range for our soil erosion rates. First, we varied the R-factor of the Adj.RUSLE model between a maximum and a minimum based on the regression equations derived by Naipal et al. (2015) per climate zone. Then we varied the C-factor of the Adj.RUSLE model between a maximum and minimum value per land cover type (tree, crop or grass) based

on literature. We then used the uncertainty range in the C and R factors to derive the uncertainty range in the soil erosion rates and subsequently in the SOC erosion rates. We performed 4 additional simulations with the emulator, 2 simulations with the setup of S1 and a minimum and maximum soil erosion scenario, and 2 simulations with the setup of S2 with a maximum and minimum soil erosion scenario. The results can be found in sections 3 and 4.

Changes in manuscript: We present the resulting soil and SOC erosion range with an uncertainty estimate that is related to the variation in the C and R factors of the Adj. RUSLE model. Furthermore, we discuss the effect of soil erosion uncertainty on the land carbon sink in section 4.4.

Global soil organic carbon removal by water erosion under climate change and land use change during 1850-2005 AD

Victoria Naipal¹, Philippe Ciais¹, Yilong Wang¹, Ronny Lauerwald^{2,3}, Bertrand Guenet¹, Kristof Van Oost⁴

¹Laboratoire des Sciences du Climat et de l'Environnement, CEA CNRS UVSQ, Gif-sur-Yvette 91191, France

7 ²Department of Geoscience, Environment & Society, Université Libre de Bruxelles, Brussels, Belgium

³Department of Mathematics, College of Engineering, Mathematics and Physical Sciences, University of Exeter, Exeter, UK

⁴Université catholique de Louvain, TECLIM - Georges Lemaître Centre for Earth and Climate Research, Louvain-la-Neuve, Belgium

Correspondence to: Victoria Naipal (victoria.naipal@lsce.ipsl.fr)

14

Abstract

21

~~Erosion is an Earth System process that transports carbon laterally across the land surface, and is currently accelerated by anthropogenic activities. The onset and expansion of agriculture has accelerated soil erosion by rainfall and runoff substantially, mobilizing vast quantities of soil organic carbon (SOC) globally. Anthropogenic land cover change has accelerated soil erosion rates by rainfall and runoff substantially, mobilizing vast quantities of soil organic carbon (SOC) globally.~~ ~~Studies show that at~~ ~~At~~ timescales of decennia to millennia this mobilized

28

SOC can significantly alter previously estimated carbon emissions from land use change (LUC). However, a full understanding of the impact of erosion on land-atmosphere carbon exchange is still missing. The aim of ~~our~~ ~~this~~ study is to better constrain the terrestrial carbon fluxes by developing methods compatible with ~~Earth System Models-Land Surface Models (LESMS)~~ ~~LESMSs~~ in order to explicitly represent the links between soil erosion by rainfall and runoff and carbon dynamics. For this we use an emulator that represents the carbon cycle of a ~~land surface model LSM~~ ~~LSM~~, in combination with the Revised Universal Soil Loss Equation model. We applied this modeling framework at the global scale to evaluate the effects of potential soil erosion (soil removal only) in the presence of other perturbations of the carbon cycle: elevated atmospheric CO₂, climate variability, and LUC. We found that over the

35

period 1850-2005 AD acceleration of soil erosion leads to a total potential SOC removal flux of ~~400 Pg C-74±18 Pg C~~ of which ~~7980-85%~~ occurs on agricultural, ~~pasture~~ and ~~natural~~ grass-lands. ~~Using our best estimates for soil erosion we find that~~ ~~including soil erosion in the SOC-dynamics scheme results in a doubling results in an increase of 62%~~ of the cumulative loss of SOC over 1850 – 2005 due to the combined effects of climate variability, increasing atmospheric CO₂ and LUC. This additional erosional loss decreases the cumulative global carbon sink on land by ~~25 Pg of carbon~~ for this specific period, with the largest effects found for the tropics, where deforestation

Comment [VN1]:

Reviewer #1: "L16: The first sentence gives me an incorrect hint that the paper is going to talk about agriculture activity accelerates soil erosion"

Answer: We agree that this may be misleading and changed this sentence.

and agricultural expansion increased soil erosion rates significantly. We ~~conclude also show~~ that the potential effects of soil erosion on the global SOC stocks ~~cannot be ignored when compared~~ is comparable to the effects of climate ~~change or land use change-LUC~~ on the carbon cycle. ~~We conclude that it~~ is thus necessary to include soil erosion in assessments of LUC and evaluations of the terrestrial carbon cycle.

1 Introduction

42

Carbon emissions from land use change (LUC), recently estimated as $1.0 \pm 0.5 \text{ Pg C yr}^{-1}$, form the second largest anthropogenic source of atmospheric CO_2 (Le Quéré *et al.*, 2016). However, their uncertainty range is large, making it difficult to constrain the net land-atmosphere carbon fluxes and reduce the biases in the global carbon budget (Goll *et al.*, 2017; Houghton and Nassikas, 2017; Le Quéré *et al.*, 2016). The absence of soil erosion in assessments of LUC is an important part of this uncertainty, as soil erosion is strongly connected to LUC (Van Oost *et al.*, 2012; Wang *et al.*, 2017).

49

The expansion of agriculture has accelerated soil erosion by rainfall and runoff significantly, mobilizing around $783 \pm 243 \text{ Pg}$ of soil organic carbon (SOC) globally over the past 8000 years (Wang *et al.*, 2017). Most of the mobilized SOC is redeposited in alluvial and colluvial soils, where it is stabilized and buried for decades to millennia (Hoffmann *et al.*, 2013a; Hoffmann *et al.*, 2013b; Wang *et al.*, 2017). Together with dynamic replacement of removed SOC by new litter input at the eroding sites, and the progressive exposure of carbon-poor deep soils, this translocated and buried SOC can lead to a net carbon sink at the catchment scale, potentially offsetting a large part of the carbon emissions from LUC (Berhe *et al.*, 2007; Bouchoms *et al.*, 2017; Harden *et al.*, 1999; Hoffmann *et al.*, 2013a; Lal, 2003; Stallard, 1998; Wang *et al.*, 2017).

56

On eroding sites, soil erosion keeps the SOC stocks below a steady-state (Van Oost *et al.*, 2012) and can lead to substantial CO_2 emissions in certain regions (Billings *et al.*, 2010; Worrall *et al.*, 2016; Lal, 2003). CO_2 emission from soil erosion can take place during the breakdown of soil aggregates by erosion and during the transport of the eroded SOC by runoff and later also by streams and rivers.

63

LUC emissions are usually quantified using bookkeeping models and ~~land surface models (LSMs)~~ that represent the impacts of LUC activities on the terrestrial carbon cycle (Le Quere *et al.*, 2016) only through processes leading to a local imbalance between NPP and heterotrophic respiration, ignoring lateral displacement. Currently, LSMs consider only the carbon fluxes following LUC resulting from changes in vegetation, soil carbon and sometimes wood products (Van Oost *et al.*, 2012; Stocker *et al.*, 2014). The additional carbon fluxes associated with the human action of LUC from the removal and lateral transport of SOC by erosion are largely ignored.

70

In addition, the absence of lateral SOC transport by erosion in LSMs complicates the quantification of the human perturbation of the carbon flux from land to inland waters (Regnier *et al.*, 2013). Recent studies have been investigating the Dissolved Organic Carbon (DOC) transfers along the terrestrial-aquatic continuum in order to better quantify CO_2 evasion from inland waters and to constrain the lateral carbon flux from the land to the ocean (Lauerwald *et al.*, 2017; Regnier *et al.*, 2013). They point out that an explicit representation of soil erosion and ~~sediment~~ transport of particulate organic matter (POC) – in addition to DOC leaching and transport - in future LSMs

is essential to be able to better constrain the flux from land to ocean. This is true, since the transfer of particulate organic carbon from eroded SOC also matters for estimating carbon inputs to rivers.

The slow pace of carbon sequestration by soil erosion and deposition (Van Oost *et al.*, 2012; Wang *et al.*, 2017) and the slowly decomposing SOC pools require the simulation of soil erosion at timescales longer than a few decades to fully quantify its impacts on the SOC dynamics. This, and the high spatial resolution that soil erosion models typically require, complicates the introduction of soil erosion and related processes in LSMs [that use short time steps \(\$\approx 30\$ min\) for simulating energy fluxes and require intensive computing resources.](#)

Previous approaches used to explicitly couple soil erosion and SOC turnover have been applying different erosion and carbon dynamic models at different spatial and temporal scales. Some studies coupled process-oriented soil erosion models with C turnover models calibrated for specific micro-catchments on timescales of a few decades to a millennium, (Billings *et al.*, 2010; Van Oost *et al.*, 2012; Nadeu *et al.*, 2015; Wang *et al.*, 2015a; Zhao *et al.*, 2015; Bouchoms *et al.*, 2017). ~~While~~ Other studies focused on the application of parsimonious erosion-SOC dynamics models using the RUSLE approach together with sediment transport methods at regional or continental spatial scales (Chappell *et al.*, 2015; Lugato *et al.*, 2016; Yue *et al.*, 2016; Zhang *et al.*, 2014). However, the modeling approaches used in these studies apply erosion models that still require many variables and data input that is often not available at the global scale or for the past or the future time period. These models also run on a much higher spatial resolution than LSMs, making it difficult to integrate them with LSMs. The study of Ito (2007) was one of the first studies to couple water erosion to the carbon cycle at the global scale, using a simple modelling approach that combined the RUSLE model with a global ecosystem carbon cycle model. However, there are several unaddressed uncertainties related to his modelling approach, such as the application of the RUSLE at the global scale without adjusting its parameters.

Despite all the differences between the studies that coupled soil erosion to the carbon cycle, they all agree that soil erosion by rainfall and runoff is an essential component of the carbon cycle. Therefore, to better constrain the land-atmosphere and the land-ocean carbon fluxes, it is necessary to develop new LSM-compatible methods that explicitly represent the link between soil erosion and carbon dynamics at regional to global scales *and* over long timescales. Based on this, our study introduces a 4D modeling approach that consists of 1) an emulator that simulates the carbon dynamics like in the ORCHIDEE LSM (Krinner *et al.*, 2005), 2) the Revised Universal Soil Loss (Adj.RUSLE) model that has been adjusted to simulate global soil removal rates based on coarse resolution data input from climate models (Naipal *et al.*, 2015), and 3) a spatially explicit representation for LUC. This approach represents explicitly and consistently the links between the perturbation of the terrestrial carbon cycle by elevated atmospheric CO₂ and variability (temperature and precipitation change), the perturbation of the carbon cycle by LUC and the effect of soil erosion at the global scale.

The main goal of our study is to use this new modeling approach to determine the potential effects of long-term soil erosion by rainfall and runoff without deposition or transport on the global SOC stocks under LUC, climate variability and increasing atmospheric CO₂ levels. In order to be able to determine if global soil erosion is a net carbon source or sink, it is essential to study first how soil erosion, without deposition or transport, interacts with the terrestrial carbon cycle. Therefore, we also aim to understand the links between the different perturbations to the

carbon cycle in the presence of soil erosion and to identify relevant changes in the spatial variability of SOC stocks under erosion.

112

2 Materials and methods

2.1 Modeling framework concept

We used the LSM ORCHIDEE-MICT (Guimberteau *et al.*, 2017; Zhu *et al.*, 2016) (in the following simply referred to as ORCHIDEE) to construct a carbon emulator that describes the carbon pools and fluxes exactly as in ORCHIDEE (Fig. 1A). MICT stands for aMeliorated Interactions between Carbon and Temperature, and this version of ORCHIDEE has several major modifications and improvements for especially the high-latitudes.

119

ORCHIDEE has 8 biomass pools, 4 litter pools, of which 2 are above-ground and 2 are below-ground and 3 SOC pools for each land cover type (Fig. 1A). It has been extensively validated using observations on energy, water and carbon fluxes at various eddy-covariance sites, and with measurements of atmospheric CO₂ concentration (Piao *et al.*, 2009). The land cover types are represented by 12 plant functional types (PFT's) and an additional type for bare soil. 10 PFT's represent natural vegetation and 2 represent agricultural land (C3 and C4 crop).

126

The turnover times for each of the PFT-specific litter and SOC pools depend on their residence time modified by local soil texture, humidity, and temperature conditions (Krinner *et al.*, 2005). ~~Land use change is not taken into account in the simulations with the full ORCHIDEE model, but is represented offline by a LUC scheme in the emulator as described in the next section. This makes it possible to switch on or off the LUC module in the emulator or to change LUC scenarios when needed without having to re-run the full ORCHIDEE model.~~ The loss of biomass and litter carbon by fire is represented by the parameterization of the Spitfire model from Thonicke *et al.* (2011) in the full ORCHIDEE model, and currently cannot be modified in our version of the emulator. Carbon losses by fire here are considered to contribute directly to the CO₂ emissions from land.

133

~~At face value, the emulator merely copies the ORCHIDEE carbon pool dynamics, and for each new atmospheric CO₂- and climate-scenario a new run of the original LSM is required to build the emulator. The emulator thus reproduces exactly the carbon pool dynamics of the full LSM. At the same time the emulator preserves the structure of the carbon cycle of ORCHIDEE and is able to reproduce the outputs exactly as by the full ORCHIDEE model.~~

The change in carbon over time for each pool of the original model is represented in the emulator by the following general mass-balance approach:

140

$$\frac{dC}{dt} = I(t) - k * C(t) \quad (1)$$

Here, $\frac{dC}{dt}$ represents the change in carbon stock of a certain pool over time, calculated by the difference between the incoming flux ($I(t)$), and the outgoing flux ($k*C(t)$) to the respective pool, where k is the turnover rate. ~~Although originally calculated by complex equations,~~ the dynamic evolution of each pool can be described using the first-order model of Eq. 1. ~~Complex equations, such as photosynthesis and hydrological processes, are needed to simulate realistically the carbohydrates input to carbon pools and the moisture and temperature conditions controlling litter and soil carbon decomposition over time. All the processes that determine surface- and soil temperature, and soil~~

Comment [VN2]:

Reviewer #2: "What are the limitations of not including these processes in the emulator? Can it capture all feedbacks and dynamics?"

Answer: Some of these processes are already included in the ORCHIDEE model, which is the basis for the C emulator but other feedbacks on SOC are missing in the original ORCHIDEE model such as the effect of SOC on the hydrology or on the thermic of the model. Nevertheless, our main objective here was to present a tool able to evaluate erosion fluxes at global scale using a 'state-of-art' land surface model outputs and estimate the drivers of erosion at global scale. In addition, this study did not focus on the feedbacks of soil erosion and land use change on NPP, the hydrological cycle or nutrient cycle and therefore it was decided not to incorporate soil erosion processes directly into ORCHIDEE, but rather use the C emulator concept instead. Not including these processes explicitly in the emulator does not change the simulated SOC dynamics in our study. However, the emulator has a flexible structure and could be made more complex depending on the needs, such as including a more sophisticated vertical discretization scheme.

The main idea of the emulator was to use a modeling tool that does not require much computational power but that still incorporates the basic processes and variables for simulating large-scale SOC dynamics under soil erosion and land use change. Many simulations were needed to quantify the various effects of soil erosion on the C cycle and to calibrate the model parameters. The C emulator was in this ...

Comment [VN3]:

Reviewer #2: "although originally calculated by complex equations, the dynamic evolution of each pool can be described using the first-order model" – why were the complex equations needed initially then? Again, what are the limitations of this first-order model?"

Answer: The limitations of this first-order model are the incapability to capture feedbacks on the hydrological processes or on the NPP (see answer to previous comment). However, because the SOC is represented by first order equations inside ORCHIDEE and the complex equations only compute the modifier to the default coefficients, and as our study focused on the effects of soil erosion on the SOC dynamics, we decided to use the C emulator, assuming that erosion will not significantly impact soil physics (and in turn decomposition) affecting SOC. The complex equations, such as photosynthesis and hydrological processes are needed to simulate realistically the changes in biomass, litter and soil respiration over time, which is done by ORCHIDEE. In the original ORCHIDEE simulations, these processes are explicitly simulated on a 30 min time step. Such a time step is needed for coupled simulations with a climate model, but makes the model CPU intensive, and there is no need for such high-resolution calculations of 'fast' C fluxes for erosion induced effects on SOC. In the emulator, all C fluxes between ecosystem compartments (with and without erosion) are exactly the same as the original ORCHIDEE, assuming that there is no feedbacks between erosion and these fluxes. The ...

147 [moisture, are calculated by the ORCHIDEE LSM on a 30 minute time-step. Such a time-step is needed for coupled](#)
[simulations with a climate model, but makes the LSM model CPU intensive. However, there is no need for such](#)
[high-temporal resolution calculations of ‘fast’ carbon and energy fluxes to account for erosion-induced effects on](#)
[SOC stocks. The addition of erosion is here supposed to impact only carbon pools, and to have no feedbacks on soil](#)
[moisture, soil temperature and photosynthesis. Therefore, we decided to use the emulator concept rather than](#)
[incorporating erosion processes directly into ORCHIDEE.](#) For each carbon pool the stock and all the incoming and
154 outgoing fluxes are derived at a daily time step from a [single](#) simulation performed with the ORCHIDEE
~~model~~ LSM. Based on the daily output stock and fluxes, the values of the turnover rates are calculated and archived
together with the input fluxes [to build the emulator. Then, the emulator can be run to simulate](#) ~~of~~ the dynamics of all
pools [over long time scales](#) without having to re-compute carbon fluxes at each time-step. [In this way the emulator](#)
reduces the computation time of the complex ORCHIDEE model significantly and allows us to easily add and study
erosion-related processes affecting the carbon dynamics of the soil. [Our main objective here is to present a tool able](#)
[to evaluate erosion-related carbon fluxes at global scale using a ‘state-of-art’ LSM output and to estimate the drivers](#)
[of carbon erosion at the global scale.](#)

161 ORCHIDEE also includes crop harvest, defined as the harvest of above-ground biomass of agricultural PFTs, and
calculated based on the concept of the harvest index (Krinner *et al.*, 2005). The harvest index is defined as the yield
of crop expressed as a fraction of the total above-ground dry matter production (Hay, 1995). ORCHIDEE uses a
fixed harvest index for crop of 0.45. However, Hay (1995) showed that the harvest index has increased significantly
since 1900 for C3 crop such as wheat. In the emulator, and also in the full ORCHIDEE model, the carbon balance of
agricultural lands is sensitive to crop harvest. Based on this we use the findings of Hay (1995) to change the harvest
168 index of C3 crops to be temporally variable over the period 1850 – 2005 in the emulator, with values ranging
between 0.26 and 0.46. This means that more crop biomass is harvested against what becomes litter. We only
changed the HI of C3 plants, because Hay (1995) mentioned that C4 plants, such as maize, had already a high HI at
the start of the last century. It should be noted that the harvest index does not vary spatially in our emulator, and
harvesting is then done constantly at each time step.

2.2 Net land use change

175 [Land use change is not taken into account in the ~~simulations with the full~~ ORCHIDEE LSM version we are using in](#)
[this study to build the emulator, but is represented by a net-land use change routine in the emulator that includes past](#)
[agricultural and grassland expansion over natural PFTs \(Fig. 1B\). This makes it possible to switch the LUC routine](#)
[on or off in the emulator or to change LUC scenarios when needed without having to re-run ORCHIDEE. We](#)
[verified that the LUC routine added to the emulator conserves the mass of all carbon pools for lands in transition to a](#)
[new land use type. When LUC takes place, the ~~To account for the effects of LUC, a net-land use change routine is~~](#)
[implemented in the emulator that includes past agricultural and grassland expansion over natural PFTs \(Fig. 1B\).](#)
182 ~~F~~ractions of PFT²s in each grid cell are updated every year given prescribed annual maps of agricultural and natural
PFTs (Peng *et al.*, 2017). The carbon stocks of the litter and SOC pools of all the shrinking PFT²s are then summed
and allocated proportionally to the expanding or new PFT²s, maintaining the mass-balance (Houghton and Nassikas,

2017; Piao *et al.*, 2009). When natural vegetation is reduced by LUC, the heartwood and sapwood biomass pools are harvested and transformed to 3 wood products with turnover times of 1 year, 10 years and 100 years. The other biomass pools (leaves, roots, sapwood below-ground, fruits, heartwood belowground) are transformed to metabolic or structural litter and allocated to the respective litter pools of the expanding PFTs (Piao *et al.*, 2009).

189 2.3 Soil carbon dynamics

The change in the carbon content of the PFT-specific SOC pools in the emulator without soil erosion can be described with the following differential equations:

$$\frac{dSOC_a(t)}{dt} = lit_a(t) + k_{pa} * SOC_p(t) + k_{sa} * SOC_s(t) - (k_{ap} + k_{as} + k_{0a}) * SOC_a(t) \quad (2)$$

$$\frac{dSOC_s(t)}{dt} = lit_s(t) + k_{as} * SOC_a(t) - (k_{sa} + k_{sp} + k_{0s}) * SOC_s(t) \quad (3)$$

$$\frac{dSOC_p(t)}{dt} = k_{ap} * SOC_a(t) + k_{sp} * SOC_s(t) - (k_{pa} + k_{0p}) * SOC_p(t) \quad (4)$$

196 ~~where~~ Where SOC_a, SOC_s, and SOC_p (g C m⁻²) are the active (unprotected), slow (physically or chemically protected) and passive (biochemically recalcitrant) SOC, respectively. The SOC pools are based on the study of Parton *et al.* (1987) and are defined by their residence times. The active SOC pool has the lowest residence time (~1.5 years) and the passive the highest (~1000 years). lit_a and lit_s (g C m⁻² day⁻¹) are the litter input rates to the active and slow SOC pools, respectively; k_{0a}, k_{0s} and k_{0p} (day⁻¹) are the respiration rates of the active, slow and passive pools, respectively; k_{as}, k_{ap}, k_{pa}, k_{sa}, k_{sp} are the coefficients determining the flux from the active to the slow pool, from the active to the passive pool, from the passive to the active pool, from the slow to the active pool and from the slow to the passive pool, respectively (Fig. 1A).

203 The SOC pools are not vertically discretized in ~~this model~~ the -version of the ORCHIDEE LSM used to build the emulator, so we implemented a simple vertical discretization scheme for the SOC pools in the emulator based on the concept of Wang *et al.* (2015a,b). In this scheme the carbon dynamics of each soil layer are calculated separately, based on layer-dependent litter input and respiration rates (Fig. 1A). The vertical discretization scheme of the emulator does not change the total input and respiration as simulated by ORCHIDEE in the case where erosion and land use change processes are switched off. We apply the same ~~vertical discretization~~ scheme for all three SOC

210 pools, assuming that ~~the each different~~ SOC pool is equally distributed across all layers of the soil profile, while ~~the ratios between the pools per soil layer are equal to those from ORCHIDEE.~~ We base this assumption on the fact that there is very little information or data to constrain the pool ratios globally, mainly because the three SOC pools cannot be directly related to measurements (Elliott *et al.*, 1996). Furthermore, neither the emulator nor the ORCHIDEE LSM model we used include soil processes that may affect these pool ratios with depth, such as vertical mixing by soil organisms, diffusion, leaching, changes in soil texture (SOC protection and stabilization by clay particles), limitations by oxygen and by access to deep organic matter by microbes. It is also uncertain how sensitive SOC is to these processes. For example, the study of Huang *et al.* (in revision for the journal *Advances in Modeling Earth Systems*) who implemented a matrix-based approach to assess the sensitivity of SOC showed that equilibrium SOC stocks are more sensitive to input than to mixing for soils in the temperate and high-latitude regions.

217

Comment [VN4]:

Reviewer #2: "What does the passive pool correspond to (as a measureable pool)? Why is there no transfer from p to s (k_{ps})? Why no input to this pool?"

Answer: The distribution of SOC into an active, slow and passive pool and the transfer rates between these pools are based on the work of Parton *et al.* (1988). These pools are defined by their different residence times. The active, slow and passive SOC pools have a residence time of 1.5, 25 and 1000 years, respectively. That study defines the passive pool as a pool that is very resistant to decomposition and includes physically and chemically stabilized SOM. The proportions of the decomposition products which enter the passive pool from the slow and active pools increase with increasing soil clay content. Passive C is thus not directly produced from litter input but active or slow C has to be stabilized first to become passive C. Then, the original model of Parton *et al.* (1988) assumes that when the passive pool is decomposed by microorganisms, they produce metabolites corresponding to more labile materials that are released in the soil solution during microbial death and the associated cell lysis. For these reasons, they considered that the decompos...

Comment [VN5]:

Reviewer #1: "I was not fully convinced by the vertical discretization approach that the emulator used. First of all, different soil layers have totally different biogeophysical and biogeochemical features. Different layers are experiencing different amount of fresh carbon input (e.g., from fine roots exudates, fine root litter), different microbial community (e.g., fungi/bacteria with different carbon use efficiency), and have different soil structure (e.g., microaggregate, macroaggregate). Secondly, even the idea of summarizing the above-mentioned vertical difference into one single factor (re) is believable, the value of re should be carefully inferred for this model, rather than taking from other studies.

Thirdly, and most importantly, the vertical discretization, artificially, increase total global SOC stock by 44%. This type of artifact should be removed. My suggestion is that, since ORCHIDEE has one single soil layer, k₀ of ORCHIDEE is supposed to represent the mean turnover rate of th...

Comment [VN6]:

Reviewer #2: "Does this allow for emergent differences in the relative distribution of the three pools with depth? (e.g., relatively more passive C than active C with depth, etc.)"

Answer: Yes, the old vertical discretization scheme allowed for different relative distributions of the three pools with depth. However, we changed this aspect by assuming that the ratios between the three pools do not change with depth so that the relative distribution is the same. We made this assumption as we have not enough data to clearly determine how the ratios between the pools change should change with depth (see reply to rev #1). In addition, we do not simulate the underlying processes that would allow for changing ratios between the SOC pools such as changing clay content with depth, diffusion, bioturbation.

~~Also, we do not include processes such as bioturbation or leaching of litter or SOC.~~

In the ~~vertical discretization scheme of the emulator~~, the soil profile is divided into thin layers of 1 cm thickness down to a depth of 2 m, which is the soil depth used by ORCHIDEE to calculate SOC. The first 10 cm of the soil profile are referred to as the “topsoil”, where we assume that the SOC content is homogeneously distributed.

224 The rest of the soil profile is referred to as the subsoil. The topsoil receives carbon from above- and below-ground litter, and each of the soil layers in the topsoil receives an equal fraction of both litter types.

The below-ground litter input for the active SOC pool is the sum of a fraction of the below-ground structural and metabolic litter pools from ORCHIDEE being re-calculated by the emulator, while the below-ground litter input for slow SOC pool is equal to a fraction of the below-ground structural litter pool only. This setting is consistent with the structure of the SOC module of the ORCHIDEE LSM to ensure that the emulator reproduces the same C pool dynamics than the LSM. The litter fractions are based on the Century model as introduced by Parton *et al.* (1987) and later implemented inside ORCHIDEE (Krinner *et al.*, 2005). We assume that the subsoil receives carbon only from below-ground litter, and that this input decreases exponentially with depth following the root profile of ORCHIDEE. This discretization of the total below-ground litter input (lit_{be}) is the same for both SOC pools and can then be represented as:

$$lit_{be} = \int_{z=0}^{z=z_{max}} I_{obe} * e^{-r*z} dz \quad (5)$$

where I_{obe} is the below-ground litter input to the surface layer, and is equal to:

$$I_{obe} = lit_{be} * \frac{r}{1 - e^{-r*z_{max}}} \quad (6)$$

238 The homogeneously distributed below-ground litter input (I_{be}) to the layers of the topsoil is equal to:

$$\frac{\sum_{z=0}^{z=10} I_{be0} * e^{-r*z}}{0.1} \quad (7a)$$

The below-ground litter input to the layers of the subsoil is equal to:

$$I_{be}(z) = I_{be0} * e^{-r*z} \quad (7b)$$

where z_{max} is the maximum soil depth equal to 2 m, and dz is the soil layer discretization (1 cm); r is the PFT-specific vertical root-density attenuation coefficient as used in ORCHIDEE.

245 The SOC respiration rates for the topsoil layers are equal to those from ORCHIDEE and are determined by average soil temperature, moisture and texture. For the rest of the soil profile the respiration rates of all three SOC pools decrease exponentially with depth:

$$k_i(z) = k_{0i} * e^{-r_e z} \quad (8)$$

Here k_{0i} is the SOC respiration rate at the surface layer for each SOC pool ($i = a, s, p$), ~~and as derived by the emulator based on the original ORCHIDEE rates.~~ r_e (m^{-1}) is an exponential decreasing coefficient representing the impact of external factors, such as oxygen availability, which reducing SOC mineralization rate with depth (z).

252 ~~After performing sensitivity simulations where the values of r_e differ per PFT, we found no significant difference in the resulting SOC stocks. The value of r_e was then set to $1.2 m^{-1}$, so that the respiration rate decreases with a factor of 2-3 from the surface to 1 m depth consistent with SOC profile observations (Bouchoms *et al.*, 2017; Van Oost *et al.*, 2005; Wang *et al.*, 2015a). This vertical discretization in the emulator leads to a total global SOC stock that is~~

Comment [VN7]:

Reviewer #2: “How are these fractions determined? What are the implications of the uncertainty in this partitioning?”

Answer: Above and below-ground litter consists out of plant residues and organic animal excreta that are partitioned into structural and metabolic pools as a function of the lignin to N ratio in the residue (Parton *et al.*, 1988). The lignin and N ratios are usually prescribed per PFT and derived from plant-trait databases. This partitioning is prescribed by Parton *et al.* (1988) and followed by Krinner *et al.* (2005). The structural litter pool has a slower decay rate and contains the more recalcitrant molecules, while the metabolic pool has a faster decay rate and contains labile plant material. The decay rates are a function of temperature and humidity (Krinner *et al.*, 2005). The lignin fraction of the plant material does not go through the active pool but is assumed to go directly to the slow C pool as the structural plant material decomposes. This is why part of the decomposed structural litter pool goes the active SOC pool and another to the slow SOC pool. Metabolic litter can be decomposed into active SOC and could also form a mineral-stabilized SOC (slow SOC pool, Cotrufo *et al.*, 2015). The CENTURY model simulates the dynamics of C and nutrients (Parton *et al.*, 1988), and is widely applied and tested in Land Surface Models. There are definitely large uncertainties in the partitioning of the litter pools, however, it is not in the scope of this paper to discuss these uncertainties.

approximately 44% larger than that from the original ORCHIDEE model, because it affects the mean value of the decomposition rates.

To ensure that the total soil respiration of the emulator is similar to that of the ORCHIDEE LSM model for each grid cell, each PFT, and each SOC pool, we have calibrated the exponent 're' and variable 'k_{0j}' of equation (8) for each grid cell and PFT under equilibrium conditions. First we selected a default value for 're' between 0 and 5, and calculated the respiration rate of the surface soil layer (k_j) when all SOC pools are in an equilibrium state, with the following equation:

$$SOC_{orchidee} = \sum_{z=0}^{z=n} \frac{L(z)}{k_{0j} e^{-re^*z}} \quad (9)$$

Where, $SOC_{orchidee}$ is the total equilibrium SOC stock derived from ORCHIDEE for a certain grid cell and PFT. $L(z)$ is the total litter input to the soil for a certain soil layer discretized according to the root profile. Then we derived the equilibrium SOC stocks per soil layer as:

$$SOC(z) = \frac{L(z)}{k_{0j} e^{-re^*z}} \quad (10)$$

Assuming that the ratios between the active, slow and passive SOC pools do not change with depth and are equal to the ratios derived from ORCHIDEE, we calculated the SOC stocks of each pool with the following equation:

$$1 + \frac{soil_s(z)}{soil_a(z)} + \frac{soil_p(z)}{soil_a(z)} = \frac{SOC(z)}{soil_a(z)} \quad (11)$$

Where, $soil_a(z)$, $soil_s(z)$, $soil_p(z)$ are the emulator derived active, slow and passive SOC stock per soil layer, grid cell and PFT. Now, for the equilibrium state the input is equal to the output, allowing us to derive k_{0a} , k_{0s} , and k_{0p} with the following equations:

$$\sum_{z=0}^{z=n} \left(\frac{L_a(z) + k_{sa} * soil_s(z) + k_{pa} * soil_p(z)}{k_{0a} * e^{-re^*z} + k_{as} + k_{ap}} \right) = SOC_a \quad (12a)$$

$$\sum_{z=0}^{z=n} \left(\frac{L_s(z) + k_{as} * soil_a(z)}{k_{0s} * e^{-re^*z} + k_{sa} + k_{sp}} \right) = SOC_s \quad (12b)$$

$$\sum_{z=0}^{z=n} \left(\frac{k_{sp} * soil_s(z) + k_{ap} * soil_a(z)}{k_{0p} * e^{-re^*z} + k_{pa}} \right) = SOC_p \quad (12c)$$

Where, L_a is the total litter input to the active SOC pool, L_s is the total litter input to the slow SOC pool. SOC_a , SOC_s , SOC_p are the total active, slow and passive SOC stocks per grid cell and PFT, respectively, derived from ORCHIDEE. k_{as} , k_{ap} , k_{sa} , k_{sp} , k_{pa} are the coefficients determining the fluxes between the SOC pools. After the derivation of 'k_{0j}' we tested if the difference in the SOC stocks between the emulator and the original ORCHIDEE LSM is less than 1 g m⁻² per grid cell and PFT. If this was not the case we increased or decreased the value of 're' and repeated the calibration cycle. If we did not find an optimized value for both 're' and 'k_{0j}' that meet this criteria, we used values that minimized the difference in SOC stocks between the emulator and the original ORCHIDEE LSM.

For the transient period (without LUC or erosion) we assumed a time-constant 're', where the values are equal to those at equilibrium. Using the mass-balance approach we calculated the daily values for k_{0a} , k_{0s} , k_{0p} per grid cell and PFT with:

$$\frac{dSOC_a}{dt} = \sum_{z=0}^n (L_a(z,t) + k_{sa} * soil_s(z,t-1) + k_{pa} * soil_p(z,t-1) - (k_{0a}(t) * e^{-re^{*z}} + k_{as} + k_{ap}) * soil_a(z,t-1)) \quad (13a)$$

$$\frac{dSOC_s}{dt} = \sum_{z=0}^n (L_s(z,t) + k_{as} * soil_a(z,t-1) - (k_{0s}(t) * e^{-re^{*z}} + k_{sa} + k_{sp}) * soil_s(z,t-1)) \quad (13b)$$

$$\frac{dSOC_p}{dt} = \sum_{z=0}^n (k_{sp} * soil_s(z,t-1) + k_{ap} * soil_a(z,t-1) - (k_{0p}(t) * e^{-re^{*z}} + k_{pa}) * soil_p(z,t-1)) \quad (13c)$$

In case there was no solution for the ' k_{0i} ' at a certain time-step we took the values from the previous time-step.

294 The annual average soil erosion rate (E , $t \text{ ha}^{-1} \text{ year}^{-1}$) is calculated by the Adj.RUSLE (Naipal et al., 2015; Naipal et al., 2016) according to:

$$E = S * R * K * C \quad (149)$$

where R is the rainfall erosivity factor ($\text{MJ mm h}^{-1} \text{ h}^{-1} \text{ year}^{-1}$), K is the soil erodibility factor ($t \text{ ha h ha}^{-1} \text{ MJ}^{-1} \text{ mm}^{-1}$), C is the land cover factor (dimensionless), S is the slope steepness factor (dimensionless). The S -factor is calculated using the slope from a 1km resolution digital elevation model (DEM) that has been scaled using the fractal method to a resolution of 150m (Naipal et al., 2015). In this way the spatial variability of a high-resolution slope dataset can be captured. The computation of the R factor has been adjusted to use coarse resolution input data on precipitation and to provide reasonable global erosivity values. For this Naipal et al. (2015) derived regression equations for different climate zones of the Köppen–Geiger climate classification (Peel et al., 2007). The results from the Adj.RUSLE model have been tested against empirical large-scale assessments of soil erosion and rainfall erosivity (Naipal et al., 2015, 2016). The original RUSLE model as described by Renard et al. (1997) also includes the slope-length (L) and support-practice (P) factors. Although these factors can strongly affect soil erosion in certain regions, the Adj.RUSLE does not include these factors due to several reasons. Firstly, (Doetterl et al., 2012) showed that these factors do not significantly contribute to the variation in soil erosion at the continental to global scales, in comparison to the other RUSLE factors. Secondly, data on the L and P factors and methods to estimate them at the global scale are very limited. Thus, including them in global soil erosion estimations would result in large uncertainties. Finally, the focus of this study is to show the effects of potential soil erosion on the terrestrial carbon cycle, without the explicit effect of management practices such as covered by the P -factor. For more information on the validation of our erosivity values and a more detailed description of the calculation of each of the RUSLE factors see supporting material section S1.

308 The Adj. RUSLE model is not imbedded in the C emulator but is run separately on a 5arcmin spatial resolution and at a yearly timestep. The resulting soil erosion rates are then read by the C emulator at each time step and used to calculate the daily SOC erosion rate of a certain SOC pool i (Ce_i in $\text{g C m}^{-2} \text{ day}^{-1}$) at the surface layer by:

$$Ce_i = SOC_i * \frac{E}{BD_{top} * dz * 10^6} \quad (150)$$

where BD_{top} is the bulk density of the surface layer (g cm^{-3}). We assume that the enrichment ratio, i.e. the volume ratio of the carbon content in the eroded soil to that of the source soil material, is equal to 1 here, which implies that our estimates of SOC mobilization are likely conservative (Chappell et al., 2015; Nadeu et al., 2015).

322 When erosion takes place, the surface layer is truncated by the erosion height, and at the same time an amount of SOC corresponding to this erosion height is removed. As we assume that the soil layer thickness does not change, part of the SOC of the next soil layer is allocated to the surface layer proportional to the erosion height and the SOC concentration (per volume) of the next layer. In this way, the SOC from all the following soil layers move upward

and become exposed to erosion in the surface layer at some point in time (Fig. 1A). To preserve mass balance, we assume that there is no SOC below the 2 m soil profile represented in the emulator and new substrate replacing the material of the last soil layer is SOC free, so that SOC in the bottom layer will decrease towards zero after erosion has started.

329

2.4 Input datasets

2.4.1 for ORCHIDEE

We used 6-hourly climate data supplied by CRU-NCEP (version 5.3.2) global database (https://crudata.uea.ac.uk/cru/data/ncep/) available at 0.5 degree resolution to perform simulations with the full ORCHIDEE model for constructing the emulator. CRU-NCEP climate data was only available for the period 1901-2012. To be able to run ORCHIDEE for the period 1850-1900, we randomly projected the climate forcing after 1900 to the years before 1900. [The random projection of the climate data is necessary to avoid the risk of including the effects of extreme climate conditions multiple times when only a certain decade is used repeatedly.](#)

336

The [historical changes of PFT fractions](#) were derived from the historical annual PFT maps ~~developed by~~ Peng *et al.* (2017). These PFT maps were available at a resolution of 0.25 degrees (Fig. 2), and were re-gridded to the resolution of the ORCHIDEE emulator, which is 2.5 x 3.75 degrees, using the nearest neighbor approach.

343

2.4.2 for the Adj.RUSLE

Due to the resolution of the Adj.RUSLE, which is 5 arcmin (~0.0833 degree), all the RUSLE factors had to be re-gridded or calculated at this specific resolution before calculating the soil erosion rates.

The land cover fractions from the historical 0.25 degree PFT maps were used in combination with the LAI values from ORCHIDEE at the resolution of 2.5° x 3.75° to derive the values for the C-factor of the RUSLE model. We first re-gridded the yearly average LAI to the resolution of the PFT maps before calculating the land cover factor of RUSLE (C-factor) at the resolution of 0.25 degree. The C values were then re-gridded using the nearest neighbor method to the resolution of the Adj.RUSLE model. We used the nearest neighbor approach here, because the C-factor is strongly dependent on the land cover class.

350

Daily precipitation data for the period 1850-2005 to calculate soil erosion rates is derived from the Inter-Sectoral Impact Model Intercomparison Project (ISIMIP), product ISIMIP2b (Frieler *et al.*, 2017). This data is based on model output of the Coupled Model Intercomparison Project Phase 5 (CMIP5 output of IPSL-CM5A-LR (Taylor *et al.*, 2012), which are bias corrected using observational datasets and the method of Hempel *et al.* (2013), and made available at a resolution of 0.5 degrees (Fig. 2). We chose this data as input to the Adj.RUSLE model, because the dataset extended to 1850, [in contrast to the CRU-NCEP data](#). Also, this dataset being bias-corrected, provides a better distribution of extreme events and frequencies of dry and wet days (Frieler *et al.*, 2017), which is important for the calculation of rainfall erosivity (R factor). The ISIMIP precipitation data was re-gridded using the bilinear

357

Comment [VN8]:

Reviewer #1: "What's the meaning of randomly projected? A more reasonable way is to repeat 1990-1910 climates during 1850-1900."

Answer: "Randomly projected", means that the climate of the years after 1900 was randomly assigned to the years between 1850 and 1900 because the climate data of CRU-NCEP was only available starting from year 1900. If we would choose to repeat the climates of 1900-1910, we would risk including the effects of extreme climate conditions multiple times.

Comment [VN9]:

Reviewer #2: "But you used CRU-NCEP for ORCHIDEE... what are the caveats of using different climate datasets for each model?"

Answer: We compared the historical trend in yearly total precipitation between CRU-NCEP and ISIMIP2b. We find that although the ISIMIP2b shows a higher overall precipitation amount, the temporal trend and variability are similar to that of CRU-NCEP. If we would use CRU-NCEP to calculate the soil erosion rates, we expect that the new soil erosion rates would fall inside the uncertainty range created by calculation of the R- and the C-factors of the Adj. RUSLE

interpolation method to the resolution of the Adj.RUSLE model, before being used to calculate the R-factor. This was necessary because the erosivity equations from the Adj.RUSLE model are calibrated at this specific resolution
364 (Naipal *et al.*, 2015).

Data on soil bulk density and other soil parameters to calculate the soil erodibility factor (K), available at the resolution of 1 km, have been taken from the Global Soil Dataset for use in Earth System Models (GSDE) (Shangguan *et al.*, 2014). The K factor has been calculated at the resolution of 1 km before being regridded to 5 arcmin using the bilinear interpolation method. We also used the SOC concentration in the soil from GSDE, which was derived using the “aggregating first” approach, to compare to our SOC stocks from simulations with the emulator. Finally, the slope steepness factor (S), which was originally estimated at the resolution of 1 km, was also
371 regridded to the resolution of 5 arcmin using the bilinear interpolation method.

Using the above-mentioned data, soil erosion rates were first calculated at the resolution of 5 arcmin, and afterwards aggregated to the coarse resolution of the emulator ($2.5^\circ \times 3.75^\circ$) to calculate daily SOC erosion rates.

2.5 Model simulations

To be able to understand and estimate the different direct and indirect effects of soil erosion on the SOC dynamics,
378 we propose a factorial simulation framework (Fig. 3 and Table 1). This framework allows isolating or combining the main processes that link soil erosion to the SOC pool, namely the influence from climate variability, LUC, and atmospheric CO₂ increase. The different model simulations described in this section will be based on this framework.

We performed two different simulations with the full ORCHIDEE model to produce the required data input for the emulator for the period 1850-2005. For this we first performed a spinup with ORCHIDEE to get steady-state carbon pools for the year 1850. We chose the period 1850-2005 based on the ISIMIP2b precipitation data availability and
385 the fact that this period underwent a significant intensification in agriculture globally and a substantial rise in atmospheric CO₂ concentrations. In the first simulation of ORCHIDEE the global atmospheric CO₂ concentration was fixed to the year 1850 to calculate time-varying NPP not impacted by CO₂ fertilization and subsequent carbon pools, while in the second simulation the atmospheric CO₂ concentration was made variable. In both simulations, climate is variable from CRU-NCEP (Fig. 3).

Furthermore, we performed ~~three~~ 7 simulations with the Adj.RUSLE model to pre-calculate the soil erosion rates that will be used as input to the ORCHIDEE emulator. Three of the 7 erosion simulations used best estimates for each model parameter, and the rest used either the minimum or maximum values for the R- and C-factors to derive an uncertainty range for our soil erosion rates and to analyze the sensitivity of the emulator. ~~to pre-calculate the soil erosion rates that will be used as input to the ORCHIDEE emulator.~~ In the first simulation with the best estimated model parameters we kept the climate and land cover variable through time (the “CC+LUC” simulation). In the second simulation we only varied the climate through time and kept land cover fractions fixed to 1850 (the “CC” simulation, Fig. 3). In the third simulation we only varied the land cover through time and kept the climate constant
392

Comment [VN10]:

Reviewer #2: “Why this dataset? How does it compare to the HWSD and SoilGrids (Hengl *et al.* PLoS ONE 2014, 2017) datasets?”

Answer: The GSDE is based on the SoilMap of the World (FAO, 1995, 2003) and various regional and national soil databases. It is available at a 1km resolution and at 5 arcmin resolution and contains updated soil information and more soil variables such as nutrients. The GSDE is based on several regional soil maps and is more up to date on soil information than the HWSD but both products compared relatively well since they shared several data (Shangguan *et al.*, 2014). We did not test the SoilGrids data, which is based on a different approach. A recent publication showed that SoilGrids give different results compared to HWSD (Tifafi *et al.*, 2018) but regarding the difference between the products we decided to use only one of them already used to evaluate erosion process and then be more comparable with previous publications (Naipal *et al.*, 2015, 2016).

399 to the average cyclic variability of the period 1850-1859 (the “LUC” simulation, Fig. 3). The erosion simulations with either minimum or maximum model parameters were either a “CC+LUC” or a “CC” type of simulation.
From the two simulations of ORCHIDEE (with variable and constant CO₂) and the 7 soil erosion simulations of the Adj.RUSLE, we constructed 4 versions of the emulator to perform 8 main simulations and 4 sensitivity simulations. The different simulations and their description are given in table 1 and figure 3. In the simulations without LUC (S2, S4, S6 and S8), the PFT fractions and the harvest index are constant and equal to those in the year 1850. In the simulations with LUC (S1, S3, S5 and S7) the harvest index increases and the PFT fraction change with time during
406 calculating the change of the carbon stocks in time depending on the perturbations during the transient period (1851-2005). In simulations with erosion, the equilibrium state of the SOC pools has been calculated using the average erosion rates of the period 1850-1859, assuming erosion to be constant before 1850 and a steady state condition where erosion fluxes are equal to new input from litter.

3 Results

413 3.1 Erosion versus no erosion

After including soil erosion in the ORCHIDEE emulator we obtain a total global soil loss flux of 47.6±10 Pg C y⁻¹ for the year 2005 of which 20 to 29% is attributed to agricultural land and 51 to 554% to grassland (natural grass and pasture). This global soil loss flux (here ‘loss’ meaning horizontal removal of SOC by erosion) leads to a total SOC loss flux of 0.52±0.1467 Pg C y⁻¹ of which 26 to 33+ are attributed to agricultural land and 54 to 640% to grassland (CTR, Fig 4). Grassland and agricultural land thus have much larger annual average soil and SOC erosion rates compared to forest (Table 2).

The total soil and SOC losses in the year 2005 are show an increase of 11-194% and 23-356.5%, respectively, compared to 1850 (CTR, Fig. 4) with the largest increases found in the tropics (Fig. 5B, D). The largest increase in soil and SOC erosion during 1850 – 2005 is found in South-America (Table 3) despite of the significant decreases in simulated precipitation leading to less intense erosion rates in this region. One should keep in mind that due to uncertainties in the simulated LUC and climate variability for certain regions and the assumptions made in our modeling framework, these trends in soil and SOC erosion rates are linked to some uncertainty. However, it is
427 difficult to assess this uncertainty, mainly due to the lack of observations for the past in regions such as the tropics and the lack of model-testing in these regions.

We found that the total soil erosion flux on agricultural land increased withby 55-58% almost doubled byin the year 2005 compared to 1850, while the SOC erosion flux increased by withby only 11-7062% (Fig. 4) and led to a cumulative SOC removal of 22±57 Pg C on agricultural land since 1850 (CTR). On pasture land and grassland, the soil erosion flux increased by only with 8-20.5%, while the SOC erosion flux increased withby 44-5434% (Fig. 4) and led to a cumulative SOC mobilization of 38±752 Pg C since 1850. It is evident that on agricultural land the uncertainty range #of soil erosion leads to a large uncertainty range in SOC erosion compared to grassland. The
434

Comment [VN11]:

Reviewer #2: How uncertain are these numbers given the model formulation assumptions, land-use maps, and methods used? It would help to see a sensitivity analysis and some uncertainty ranges.

Answer: We performed 4 additional simulations with a different PFT map, which is also based on the LUH2 land use dataset but where the historical forest area change that is not constrained by data as done by Peng et al. (2017). We used these simulations to show the differences to our results when other land use maps are used. If the forest is not constrained with methods described by Peng et al. (2017), there is a stronger decrease in forest area over the period 1850-2005. Also the grassland shows an increasing trend, while in the PFT map with constrained forest the grassland shows globally a slight decreasing trend. In the rest of the text we will refer to the PFT map constrained with data on forest area as the ‘constrained PFT map’ and to the other PFT map as the ‘unconstrained PFT map’. Differences in global average soil erosion rates between the different PFT maps are small, however, there are significant differences in the SOC erosion rates and cumulative changes in SOC stocks during the transient period. According to the unconstrained PFT map, soil erosion leads to a total SOC removal of 79 Pg (simulation S1 with the new vertical discretization scheme) over the period 1850-2005, which is 6Pg larger than the total SOC removal by soil erosion under the constrained PFT map. Interestingly, according to the unconstrained PFT map, the global cumulative SOC stock change over 1850-2005 under soil erosion and LUC (S1) is 60% smaller than the stock derived using the constrained PFT map. This is most likely due to the higher forest area at the start of the period 1850-2005, leading to a larger increase in SOC stocks by increasing atmospheric CO₂ concentrations. The global LUC effect on the SOC stocks of both PFT maps is found to be similar. For more details and our changes in the manuscript see our answer to comment 2 of reviewer 1.

We also derived an uncertainty range for our soil erosion rates. First, we varied the R-factor of the Adj.RUSLE model between a maximum and a minimum based on the regression equations derived by Naipal et al. (2015) per climate zone. Then we varied the C-factor of the Adj.RUSLE model between a maximum and minimum value per land cover type (tree, crop or grass) based on literature. We then used the uncertainty range in the C and R factors to derive the uncertainty range in the soil erosion rates and subsequently in the SOC erosion rates. We performed 4 additional simulations with the emulator, 2 simulations with the setup of S1 and a minimum and maximum soil erosion scenario, and 2 simulations with the setup of S2 with a maximum and minimum soil erosion scenario.

441 ~~increase in SOC erosion is much larger than the increase in soil erosion on for grasslands because in our model, LUC (without erosion) leads to a significant increase in SOC on grassland amplifying the increasing trend in SOC erosion for grassland. SOC erosion increases less strongly during 1850–2005 compared to soil erosion, while on grassland the opposite effect is true. This is because in our model, LUC (without erosion) leads to a significant increase in SOC on grassland, which amplifies the increasing trend in SOC erosion for grassland. This simulated increase for in~~
SOC stocks on grasslands after LUC ~~takes place~~ is not unrealistic, as it is observed from paired chronosequences worldwide ~~that where~~ grasslands have higher SOC densities than forests for instance (Li *et al.*, 2017).

In total 7183 ± 1662 Pg of soil and 74 ± 18400 Pg of SOC is mobilized across all PFTs by erosion during the period 1850 - 2005, which is equal to approximately ~~46-7480%~~ of the total net flux of carbon lost as CO₂ to the atmosphere due to LUC (net LUC flux) over the same period estimated by our study (S1-S2). In this study, we do not address the fate of this large amount of eroded SOC, be it partly sequestered (Wang *et al.*, 2017) or released to the atmosphere as CO₂.

448 ~~To estimate the net effect of soil erosion on the global SOC stocks under all perturbations we compare the cumulative SOC stock change from simulation S3 (no erosion; see Table 1) with that of the CTR simulation. When assuming that the SOC mobilized by soil erosion in the CTR simulation is all respired (this is certainly an extreme and unrealistic assumption, as case in reality a fraction of mobilized SOC will remain stored on land, but we take this assumption as an extreme scenario) we find that the overall global SOC stock decrease would almost double during the period 1850–2005 compared to a world without soil erosion (Fig. 6A). The largest impact of including erosion in the SOC modeling scheme is observed for Asia, where the decrease in the total SOC stock is 9 times larger when the effects of soil erosion are taken into account (Table 4, Fig. 8A). Some regions, such as West Europe show instead a smaller SOC loss when erosion is taken into account. This is because we assume a steady state in 1850, where carbon losses by erosion are equal to the carbon input by litter. And as soil erosion decreased during 1850–2005 for Western Europe, mainly due to a decreasing trend in precipitation since 1965 and less intense expansion of agricultural and grasslands (Fig. 5B), it partly offsets the decrease of SOC by LUC (Fig. 8).~~

Comment [VN12]: This part is moved to the discussion paragraph 4.1

3.2 Validation of model results

462 We calculated a total global SOC stock for 2005 in the absence of soil erosion (S3) of 12842589 Pg ~~C~~, which is a factor of $0.731-48$ ~~lower~~ ~~higher~~ than the total SOC stock from GSCE (Shangguan *et al.*, 2014) for a soil depth of 2m (Table 5). SOC stocks of forest in our model contribute the most to this overestimation. ~~We find that SOC stocks of agricultural land show the best comparison to the stocks of the GSCE dataset (Table S3).~~ Including soil erosion (S1, ~~minimum, maximum~~) leads to a total SOC stock of 1001 ± 58936 Pg ~~C~~ for the year 2005 (Table 5). We also find that including soil erosion in the SOC-dynamics scheme slightly improves the root mean square error (RMSE) between the simulated SOC stocks and those from GSCE, for the top 30cm of the soil profile. This improvement in
469 the RMSE occurs especially in highly erosive ~~regions~~ ~~areas~~. ~~However, there are still large differences between our simulated SOC stocks and those from GSCE due to large uncertainties in the simulation of underlying processes that govern the SOC dynamics (Todd Brown et al., 2014) and missing SOC transport and deposition after erosion.~~

476 Furthermore, the total SOC stock of agricultural land is significantly lower than [that](#) of the GSDE, because we
assume a steady-state landscape at 1850, where soil erosion losses are equal to the carbon input to the soil. [We](#)
[abstained](#) ~~did not perform~~ [from a more in-depth comparison with SOC global observations as our emulator and the](#)
[original ORCHIDEE LSM do not include various soil processes that have been proven to affect SOC substantially](#)
483 [such as vertical mixing, diffusion, priming, changes in soil texture, carbon rich organic soils formation, etc. The](#)
[ORCHIDEE LSM model we use to build the emulator also lacks processes such as nitrogen and phosphorus](#)
[limitations and priming, which affect the productivity and SOC decomposition \(Goll *et al.*, 2017; Guenet *et al.*,](#)
[2016\). The emulator also](#) ~~misses~~ [simulates only the removal of SOC but not the subsequent SOC transport and](#)
[deposition after erosion, and there is a general uncertainty in the simulation of underlying processes that govern the](#)
[SOC dynamics \(Todd-Brown *et al.*, 2014\). Finally, large uncertainties in the global soil databases \(Hengl *et al.*,](#)
[2014; Scharlemann *et al.*, 2014; Tifafi *et al.*, 2018\), complicate the exact quantification of the uncertainties of the](#)
[resulting SOC dynamics simulated by our emulator.](#)

Using the Adj.RUSLE model to estimate agricultural soil loss by water erosion for the year 2005 resulted in a global
soil loss flux of 12.28 ± 4.624 Pg y^{-1} (Fig. 4). This flux is paralleled by a SOC loss flux of 0.16 ± 0.069 Pg C y^{-1} after
including soil erosion in the CTR simulation (Fig. 4). This soil loss flux is in the same order of magnitude as earlier
high-resolution assessments of this flux, while the SOC removal flux is slightly lower compared to previously
published high-resolution estimates, but within the uncertainty (Table 6). We also find a fair agreement between our
490 model estimates of recent agricultural soil and SOC erosion fluxes per continent and the high-resolution estimates
(excluding tillage erosion) from the study of Doetterl *et al.* (2012) (Table 7). However, the continental SOC erosion
fluxes from our study are generally lower, because of the lower SOC stocks on agricultural land. Only South-
America shows a higher SOC flux for present-day compared to the high-resolution estimates of Doetterl *et al.*
(2012), which is the result of the simulated high productivity of crops in the tropics.

Furthermore, we find a cumulative soil loss of 1888 ± 753 Pg and cumulative SOC removal flux of 22 ± 57 Pg C from
agricultural land over the entire time period (CTR simulation). This soil loss flux lies in the range of 2480 ± 720 Pg
497 found by Wang *et al.* (2017) for the same time period, while the SOC removal flux is significantly lower than the 63
 ± 19 Pg C found by Wang *et al.* (2017). Wang *et al.* (2017) used only recent climate data in his study while we
explicitly include the effects of changes in precipitation and temperature on global soil erosion rates and the SOC
stocks in our study, which may explain this difference.

4 Discussions

504 4.1 Significance of including soil erosion in the ORCHIDEE emulator

[To estimate the net effect of soil erosion on the global SOC stocks under all perturbations we compare the](#)
[cumulative SOC stock change from simulation S3 \(no erosion; Table 1\) with that of the CTR simulation with all](#)
[factors included, that is, land use, CO₂, and climate. When considering our best estimated soil erosion rates and](#)

Comment [VN13]:

Reviewer #2: "The emulator used in this study seems to have various limitations that make the numbers presented quite uncertain – further discussion on, and quantification of, these uncertainties is warranted and would greatly improve this manuscript. Specifically, I would have liked to see additional support for the SOC model formulation, parameters, and built-in feedbacks chosen for the emulator, as well as support for its vertical discretization and parameterization. The carbon emulator is supposed to describe the carbon pools and fluxes exactly as in ORCHIDEE, yet the total global SOC stocks from the emulator are 44% higher than that of the original ORCHIDEE model. This is a big difference. What does this tell us about the accuracy and applicability of the emulator, and how do the SOC stocks of the two models compare to the Harmonized World Soil Database (HWSO) and other global SOC databases? Additional major comments/questions, especially those regarding the assumptions and methods used, are detailed below."

Answer: We modified the vertical discretization scheme of the emulator in such a way that the total SOC stock of each grid cell, PFT and C pool is close to that of ORCHIDEE when soil erosion and land use change is deactivated (0.5% max difference in total global SOC stock). For this we calibrated both the exponent '*re*' and variable '*k_{oi}*' of equation 8 in the manuscript for each grid cell and PFT under equilibrium conditions, such that the total soil respiration per grid cell, PFT, and soil C pool of the emulator would be similar to that of the ORCHIDEE model. For the transient period (1850-2005), we made '*re*' remain equal to the equilibrium state values, while values for '*k_{oi}*' were derived at a daily time-step to keep to SOC stocks of the emulator similar to those of ORCHIDEE and preserve the yearly variability in the soil respiration rates due to changes in soil climate (soil erosion and land use change were deactivated). Details of how we calibrated the exponent '*re*' and variable '*k_{oi}*' we describe in our response to Reviewer 1. The

Comment [VN14]:

Reviewer #2: "(Section 4.4) with all of these model limitations, it would be nice to have a rough quantification of uncertainties."

Answer: We agree with the reviewer that quantifying the uncertainty is important. Therefore, we derived an uncertainty range for our soil erosion rates. First, we varied the R-factor of the Adj.RUSLE model between a maximum and a minimum based on the regression equations derived by Naipal *et al.* (2015) per climate zone. Then we varied the C-factor of the Adj.RUSLE model between a maximum and minimum value per land cover type (tree, crop or grass) based on literature. We then used the uncertainty range in the C and R factors to derive the uncertainty range in the soil erosion rates and subsequently in the SOC erosion rates. We performed 4 additional simulations with the emulator, 2 simulations with the setup of S1 and a minimum and maximum soil erosion scenario, and 2 simulations with the setup of S2 with a maximum and minimum soil erosion scenario. The results can be found in chapter 3 and 4.

511 [assuming that the SOC mobilized by soil erosion in the CTR simulation is all respired, we find an overall global](#)
[SOC stock decrease that is 62 % larger compared to a world without soil erosion during the period 1850 – 2005](#)
[\(Fig. 6A\). This assumption is certainly an extreme and unrealistic assumption, as in reality a fraction of the](#)
[mobilized SOC will remain stored on land, but we take this assumption as an extreme scenario. Including soil](#)
[erosion in the SOC cycling scheme under the previously mentioned assumption thus reduces the global land C sink](#)
[with the largest impact observed for Asia, where the decrease in the total SOC stock is 156% larger when the effects](#)
[of soil erosion are taken into account \(Table 4, Fig. 8A\). Some regions, such as Western Europe show instead a](#)
[smaller SOC loss when erosion is taken into account. This is because we assumed a steady state in 1850, where](#)
518 [carbon losses by erosion are equal to the carbon input by litter. And as soil erosion decreased during 1850 - 2005 in](#)
[Western Europe, mainly due to a decreasing trend in precipitation since 1965, less intense expansion of agricultural-](#)
[and grasslands \(Fig. 5B\) and agricultural abandonment, it partly offsets the decrease of SOC by LUC \(Fig. 8\).](#)

The significantly smaller increase in SOC stocks on agricultural land when [the best estimated](#) soil erosion [rates](#) ~~are~~
taken into account (Fig. 7) explains the ~~much higher~~ [larger](#) decrease in the global SOC stock during 1850 – 2005
[\(S1\)](#) compared to a world without soil erosion (Fig. 6A). Due to the slow response of the global SOC stocks to
525 perturbations, this impact of soil erosion can be even larger at longer timescales. The effect of soil erosion on the
SOC stocks is also influenced by the mechanism where removal of SOC causes a sink in soils that tend to return to
equilibrium.

Furthermore, we find that the variability in the temporal trend of global SOC erosion is mainly determined by the
variability in soil erosion rates and less by climate and rising atmospheric CO₂ that are affecting SOC stocks (Fig. 4).
Also the spatial variability in SOC erosion rates for the year 2005 and the spatial variability in the change of SOC
erosion during 1850 – 2005 follow closely the spatial variability of soil erosion rates (Fig. 5B, D). This can be
explained by the slow response of the SOC pools to changes in NPP and decomposition caused by CO₂ and climate
in contrast to the fast response of soil erosion to changes in land cover and climate.

532

4.2 LUC versus precipitation and temperature change

Although the variability in the temporal trends of soil and SOC erosion is dominated by the variability in
precipitation changes, the overall trend follows the increase in agricultural land and grassland. [The global decrease](#)
[in precipitation in many regions worldwide, especially in the Amazon, as simulated by ISIMIP2b, leads to a slight](#)
539 [decrease in soil and SOC erosion rates \(Fig. 4\). At the same time precipitation is very variable and might not lead to](#)
[a significant global net change in soil erosion rates over the total period 1850-2005. This result might be](#)
[contradictory to the fact that major soil erosion events are caused by storms. But in this study we only simulate rill](#)
[and interrill erosion, which are usually slow processes. In addition, previous studies \(Lal, 2003; Montgomery, 2007;](#)
[Van Oost et al., 2007\) have shown that land use change is usually the main driver behind accelerated rates of these](#)
[types of soil erosion. Our study confirms this observation.](#)

If we separate the effects of LUC and climate variability co-varying with soil erosion we find that in the “LUC”
erosion scenario with constant climate (see section 2.5), the total global soil loss from erosion increases by a factor

546 | of 1.27 since 1850, while in the “CC” erosion scenario with constant LUC [at the level of 1850](#) the soil loss flux from erosion decreases by a factor of 1.12 (Fig 4). Analyzing the effects of LUC and climate variability separately on SOC erosion we find that in the LUC-only scenario (S2-S1) the total global SOC loss increases by a factor of 1.35 since 1850, while in the climate-change-only scenario (S2) SOC loss decreases by a factor of 1.12 (Fig 4). This shows that LUC slightly dominates the trend in both soil and SOC erosion fluxes on the global scale during 1850 - 2005.

553 | For soil erosion, however, LUC dominates the temporal trend less than for SOC erosion. This effect is especially clear for grasslands, where we find that climate variability offsets a large part of the increase in soil erosion rates by LUC, but not in the case of SOC erosion. This is due to the fact that LUC has a much stronger effect on the carbon content in the soil than the effect of climate and CO₂ change on the timescale of the last 200 years. Also, intense soil erosion is typically found in [mountainous areas](#) where climate variability has significant impacts, while at the same time these regions are usually poor in SOC [due to unfavorable environmental conditions for plant productivity](#).

560 | Regionally, there are significant differences in the relative contributions of LUC versus climate variability to the total soil erosion flux (Fig. 2 & 5). In the tropics in South-America, Africa and Asia, where intense LUC (deforestation and expansion of agricultural areas) took place during 1850 - 2005, a clear increase in soil erosion rates is found even in areas with a significant decrease in precipitation due to a higher agricultural area being exposed to erosion. However, in regions where agriculture is already established and has a long history, precipitation changes seem to have more impact than LUC on soil erosion rates. A combination of our assumption that erosion rates are in steady state with carbon input to the soil at 1850, and minimal agricultural expansion during the last 200 years may be the reasons for this observation.

567 | We also find that summing up the changes in soil erosion rates due to LUC alone and the changes in soil erosion due to climate variability alone do not exactly match the results in the changes in soil erosion obtained when LUC and climate variability are combined (Fig. 4). The non-linear differences between soil erosion rates calculated with changing land cover fractions in combination with a constant climate (“LUC”), and soil erosion rates calculated by subtracting the erosion simulation “CC” from “CC+LUC” are significant for agricultural land but much smaller for other PFTs and at the global scale. It implies that the LUC effect on erosion depends on the background climate. This is important to keep in mind when evaluating the LUC effect on SOC stocks in the presence of soil erosion.

574 | The decrease in global SOC stocks in simulation S3 are due to the various effects of LUC (without erosion) (Fig. 6A). During 1850 – 2005 LUC has led to a decrease in natural vegetation and an increase in agricultural land. At the global scale, the replacement of natural PFTs by crop results in increased SOC decomposition and decreased carbon input to the soil by litter-fall due to harvest and a lower productivity. [Regionally this effect](#) of LUC may be different, depending for example on the natural PFTs that are replaced. Furthermore, the increase in carbon input into the soil after LUC due to increased litter fall when natural vegetation is removed may play a role, but this effect is only temporary. In addition, wood harvest after deforestation and crop harvest contribute to the decreased carbon input to
581 | the soils.

Comment [VN15]:

Reviewer #1: “Also, intense soil erosion is typically found in mountainous areas where climate variability has significant impacts, while at the same time these regions are usually poor in SOC.” It’s not clear in the manuscript whether or not ORCHIDEE has topography information? In another word, if ORCHIDEE simulates a low SOC stock over the grid cells that have mountains, is that because of the topographical feature of this gridcell can not hold a lot of SOC in ORCHIDEE? Or because of other reasons such as climate constraints (e.g., colder in mountain area)?”

Answer: ORCHIDEE has no soil depth information and thus cannot simulate low SOC stocks due to the fact that the gridcell cannot hold a lot of SOC. Low SOC might however be a result of the plant productivity, the climate (temperature and precipitation), soil moisture and clay content (which is a constant variable). ORCHIDEE has, however, topographical information such as slope that determines the flow directions for water/runoff and affects hydrological parameters such as soil moisture content.

Comment [VN16]:

Reviewer #1: “CO₂ fertilization effects on NPP is not fully convincing here, because ORCHIDEE does not have nutrient constraints. OCN might be a better surrogate model to be able to say something about CO₂ fertilization effect on NPP.”

Answer: In the ORCHIDEE model version we used the nutrients are indeed absent. Our intention, however, was to show the complete picture of possible direct and indirect interactions of soil erosion with the C cycle with the current model setup. The representation of nutrients in global land surface models is new and the related uncertainties are not well quantified. We work with a more or less simple version of ORCHIDEE and the C emulator to be able to understand and quantify the effects of soil erosion on the C cycle. We mention the uncertainties due to the absence of nutrients in the next chapter.

We find that ~~the global~~ ~~by the~~ SOC stocks decreases by ~~1734~~ Pg C due to LUC only during 1850 – 2005 (Fig. 6A, S3-S4). The overall change in carbon over this period summed up over all biomass, litter, SOC, and wood-product pools due to LUC without erosion is a loss of ~~10248~~ Pg C, which lies in the range of cumulative carbon emissions by LUC from estimates of previous studies (Houghton and Nassikas, 2017; Li et al., 2017; Piao et al., 2009). When we use our best estimated soil erosion rates in the SOC-dynamics scheme of the emulator we find that the LUC effect on the global SOC stock is amplified by 4 Pg C or a factor of 1.2 (S1-S2, Fig. 6A). The main reason behind this is the increase in soil erosion rates by expanding agricultural- and grasslands that limits the increase in the global agricultural and grassland SOC stock due to LUC (Fig. 7). (S1-S2) amplifies the decrease of SOC stocks implied by LUC in absence of erosion (S3-S4) by 7 Pg or a factor of 1.2 (Fig. 6A). This leads to a total change in the overall carbon stock on land due to LUC of ~~-10265~~ Pg. Regionally the amplification of the LUC effect on SOC stocks by the increase in soil erosion ranges between factor of 0.9 and 1.6 (Table 4).

Regionally, changes in precipitation can amplify or offset a large part of the increase in soil erosion due to LUC (Fig. 2 & 5E). Globally we find that the decrease in global total precipitation, especially in the Amazon after 1960AD, partly offsets the increase in soil loss due to land use change (Fig. 4). It should be noted that the uncertainty in precipitation from global climate models for the Amazon is significant making this result uncertain (Mehran *et al.*, 2014). Furthermore, we find that precipitation and temperature changes lead to a small net decrease in SOC stocks at the global scale since 1950 (Fig. 9, S8). This is likely related to the decreased productivity under drought stress (Piao *et al.*, 2009). However, soil erosion offsets this decrease by a small net increase of 2 Pg in SOC stocks, mostly due to the decreasing trend in precipitation globally after 1950 AD.

602 4.3 Effects of atmospheric CO₂ increase

In the ORCHIDEE model, increasing CO₂ leads to a fertilization effect as it increases the NPP, and results in a significant increase in biomass production on land for most PFTs, depending on the temperature and moisture conditions (Arnoeth *et al.*, 2017; Piao *et al.*, 2009). Figure 9 shows the contribution of this fertilization effect to the cumulative SOC stock change during 1850 – 2005 (S4-S8), which is in the same order of magnitude as the effect of LUC excluding soil erosion. Together with climate variability the atmospheric CO₂ increase offsets all the carbon losses by LUC in our model, and leads even to a net cumulative sink of carbon on land over this period of about ~~3028~~ Pg C (S3). This value is calculated by summing up the changes in all the biomass, litter and SOC pools, and is in line with other assessments that found a net carbon balance that is close to neutral over 1850 - 2005 (Arora *et al.*, 2011; Ciais *et al.*, 2013; Khatiwala *et al.*, 2009).

In the presence of soil erosion, climate variability and the atmospheric CO₂ increase lead to a ~~slightly smaller~~ net cumulative sink of carbon over land of about 283 Pg C (S1), still within the uncertainty of assessed estimates (Arora *et al.*, 2011; Ciais *et al.*, 2013; Khatiwala *et al.*, 2009). Soil erosion can thus slightly change the sink strength by influencing the net effect of LUC on the terrestrial carbon balance.

When the CO₂ fertilization effect is absent (S5, S7), we find that the temporal trend in the cumulative change of global SOC stocks is largely determined by the effect of LUC (Fig. 6B), and leads to a cumulative source of carbon on land of ~~9276~~ Pg C. LUC alone leads to a cumulative decrease in SOC stocks of ~~-1429~~ Pg C (S7-S8), which is ~~35~~ Pg C less than the decrease in SOC stocks due to LUC in the presence of increasing atmospheric CO₂ concentrations (S3-S4). The overall change in carbon over 1850-2005 summed up over all biomass, litter and SOC pools due to LUC alone is ~~-9974~~ Pg C in absence of increasing CO₂ (S7-S8), which is ~~2479~~ Pg C less than the LUC effect on carbon stocks under variable atmospheric CO₂ (S3-S4). LUC has indeed a smaller effect on carbon stocks in the absence of increasing CO₂ concentrations as expected, because the productivity of the vegetation is lower (lower NPP) resulting in less biomass that can be removed by deforestation.

The previously calculated global total soil erosion flux of 47.6 Pg y⁻¹ leads to an annual SOC erosion flux of ~~0.486±0.135~~ Pg C y⁻¹ in the year 2005 in the absence of increasing atmospheric CO₂ (S5), which is about 0.042 Pg C y⁻¹ less than the SOC erosion flux under increasing CO₂ (S1). The global cumulative SOC ~~loss-erosion~~ over the entire time period in the absence of increasing atmospheric CO₂ is about 4.78 ± Pg C less (S5). Although these changes in SOC are small, the effect of LUC on the SOC stocks is amplified by erosion with a factor of 1.267 in absence of increasing CO₂ (S5-S6), which is significantly larger than the effect of LUC with increasing CO₂ (S1-S2). This means that the LUC effect in combination with soil erosion has a stronger effect on SOC stocks losses under constant atmospheric CO₂ conditions, because the CO₂ fertilization effect does not replenish SOC in agricultural lands everywhere.

Finally, it should be mentioned here that the absence of nutrients in the current version of the ORCHIDEE model may result in an overestimation of the CO₂ fertilization effect on NPP and may introduce biases in the effect of erosion on SOC stocks under increasing atmospheric CO₂ concentrations. Soil erosion may also lead to significant losses of nutrients in the real world, especially in agricultural areas. For a more complete quantification of the effects of soil erosion on the carbon cycle, nutrients have to be included in future studies.

644 4.4 Model limitations, uncertainties and next steps

One of the uncertainties ~~related to~~ in our modeling approach is related to the application of the Adj. RUSLE model at the global scale and the estimation of the model parameters for various different environmental conditions and biomes. Although the Adj. RUSLE model was extensively validated using large high-resolution datasets, we calculated an uncertainty range for the R and C factors of the model to investigate the sensitivity of the emulator to the uncertainty in soil erosion rates. In section 4.1 we show that including soil erosion in the emulator decreases the land carbon sink due to the large SOC losses on agricultural land triggered by erosion that reduce the SOC stocks significantly. Without soil erosion (S3) the global agricultural SOC stock increases by 60 Pg C due to agricultural expansion, while soil erosion reduces this increase by 11 Pg C in the minimum soil erosion scenario (S1 minimum) and by 18 Pg C in the maximum soil erosion scenario (S1 maximum). LUC results thus in a smaller increase in the

global agricultural SOC stock under all soil erosion scenarios, while the magnitude of this effect is region-dependent. The larger the soil erosion rates, the lesser carbon can be stored on agricultural land.

Furthermore, the aggregation of the high-resolution soil erosion rates from the Adj.RUSLE model to the resolution of the emulator can induce some uncertainties, ~~which is needed because of the coarse resolution of ORCHIDEE and the limited computational power.~~ In this way, as we might not capture correctly the hotspots of carbon erosion and their effects on the local SOC dynamics in these regions. However, the aggregation was needed to be consistent with the coarse resolution of ORCHIDEE and the limit the computational power of the emulator.

In addition, our soil erosion model is limited to water erosion only. This might result in biases for regions where other types of soil erosion are dominant such as, tillage erosion (Van Oost *et al.*, 2007), gully erosion and landslides (Hilton *et al.*, 2008; Hilton *et al.*, 2011; Valentin *et al.*, 2005).

Although our erosion model runs on a daily time step, the soil erosion rates are calculated on a yearly time step, and thus we might miss extreme climate events triggering large soil losses. In addition, the Adj.RUSLE is not trained for extreme events. The effect of precipitation and temperature change on the SOC stocks under soil erosion might thus be larger than in our model simulations.

Concerning the reconstructed PFT maps, only expansion and abandonment of agriculture is taken into account, but not soil conservation measures as implemented in Australia and the US to prevent erosion (Chappell *et al.*, 2012; Houghton *et al.*, 1999). Regarding the land use change method that we applied, we only account for net land use change and do not account for shifting cultivation or distinguish between areas that have already seen LUC. Forest regrowth and forest age are also not considered, which could bring uncertainties in our estimates of LUC emissions (Yue *et al.*, 2017).

To show the potential uncertainty in our results due to uncertainties in underlying land use data we performed 4 additional simulations (S1 to S4) with a new PFT map using the same methods and data as by Peng et al. (2017), however, where the forest area is not constrained with historical data from Houghton (2003, 2008) and present-day data from satellite land-cover products. In the following we will refer to the new PFT map as the unconstrained PFT map. In the unconstrained PFT map there is a stronger decrease in forest area over the period 1850-2005. Also the grassland shows an increasing trend, while in the PFT map with constrained forest the grassland shows globally a slight decreasing trend (Fig. S2 of the supporting material).

After calculating soil erosion with the unconstrained PFT map we find that the differences in global average soil erosion rates between the different PFT maps are small (Fig. S3A in the supporting material). This can be related to the fact that the C-factor of the Adj. RUSLE model is similar for forest and dense natural grass. As the change in global agricultural area is not significantly different between the two PFT maps, the overall soil erosion rates are similar. We expect, however, that the differences in soil erosion rates between the PFT maps can be larger in areas where the change in forest area is substantial over the historical period.

In contrast to the soil erosion rates, the two PFT maps result in significant differences in the SOC erosion rates and cumulative changes in SOC stocks during the transient period (Fig. S4 of the supporting material). The global SOC stock in the equilibrium state without soil erosion (S3) is 8 % higher when the unconstrained PFT map is used, due to a larger global forest area in this map at 1850. The higher global SOC stock of the unconstrained PFT map leads to higher SOC erosion rates (Fig. S3 B in the supporting material). According to the unconstrained PFT map, soil

Comment [VN17]:

Reviewer #1: "Land use change map. The LUC is prescribed by PFT fractional change derived from Peng 2017. Wondered how this LUC dataset differs from Land-Use Harmonization (LUH2), the new CMIP6 land use change dataset. Given that LUC is a dominant factor of SOC erosion, I am curious about the uncertainty of SOC erosion, induced by using different LUC estimate (e.g., Peng 2017 vs LUH2)."

Answer: The PFT fractional map is based on LUHv2 land use dataset, historical forest area data from Houghton (for large regions) and present day forest area from ESA CCI satellite land cover data (Peng et al., 2017). The historical forest data from Houghton and the latest satellite land cover data from ESA are the best estimates that currently exist on forest area. Figure S... shows that if the forest is not constrained with methods described by Peng et al. (2017), there is a stronger decrease in forest area over the period 1850-2005. Also the grassland shows an increasing trend, while in the PFT map with constrained forest the grassland shows globally a slight decreasing trend. In the rest of the text we will refer to the PFT map constrained with data on forest area as the 'constrained PFT map' and to the other PFT map as the 'unconstrained PFT map'.

We agree with the reviewer that different land use data can result in large uncertainties in both SOC stocks and soil erosion rates. To show the potential uncertainty in our results due to uncertainties in underlying land use data we performed 4 additional simulations (S1 to S4) using the unconstrained PFT map and the new vertical discretization scheme. The results are described here in the revised manuscript.

erosion leads to a total SOC removal of 79 Pg C (S1) over the period 1850-2005, which is 5 Pg C larger than the total SOC removal by soil erosion for the constrained PFT map.

693 Interestingly, due to the unconstrained PFT map, the global cumulative SOC stock change over 1850-2005 under soil erosion, climate change and LUC (S1) is 60% smaller than the stock derived using the constrained PFT map. This is most likely due to the higher forest area at the start of the period 1850-2005, leading to a larger increase in SOC stocks by increasing atmospheric CO₂ concentrations. We find the global LUC effect on the SOC stocks of both PFT maps to be similar (Fig. S3 C and D in the supporting material).

700 Finally, the ORCHIDEE model lacks processes such as nitrogen and phosphorus limitations and priming, which affect the productivity and SOC decomposition (Goll *et al.*, 2017; Guenet *et al.*, 2016).

Comment [VN18]: Moved to chapter 3.2

5 Conclusions

In this study we introduced a 4D modeling approach where we coupled soil erosion to the C-cycle of ORCHIDEE and analyzed the potential effects of soil erosion, without sediment deposition or transport, on the global SOC stocks over the period 1850 – 2005. To calculate global potential soil erosion rates we used the Adj.RUSLE model that includes scaling approaches to calculate soil erosion rates at a coarse spatial and temporal resolution. The SOC dynamics are represented by an emulator that imitates the behavior of the carbon cycle of the ORCHIDEE LSM and enables us to easily couple our soil erosion model to the C-cycle and calculate the effects of soil erosion under different climatic and land use conditions. Although our modeling approach is rather coarse and fairly simple, we found a fair agreement of our soil loss and SOC loss fluxes for the year 2005 with high-resolution estimates from other studies.

707 When applying the model on the time period 1850-2005 we found a total soil loss flux of 7183±1662, where soil erosion rates increased strongest on agricultural land. This potential soil loss flux mobilized 74±18400 Pg of SOC across all PFTs, which compares to 46-7480% of the total net flux of carbon lost as CO₂ to the atmosphere due to LUC estimated by our study for the same time period. When assuming that all this SOC mobilized is respired we find that the overall SOC change over the period 1850-2005 would increase by 62% and reduce the land carbon sink by 2 Pg of C double. The effect of soil erosion on the cumulative SOC change between 1850 and 2005 AD differs significantly between regions, where the largest decrease in SOC due to soil erosion is found in Asia. The expansion of agricultural and grassland is the main driver behind the decreasing SOC stocks by soil erosion. Including soil erosion in the SOC dynamics amplifies the decrease in SOC stocks due to LUC by a factor of 1.2.

714 Overall, the potential effects of soil erosion on the global SOC stocks show that soil erosion needs to be included in future assessments of the terrestrial C-cycle and especially LUC.

Data availability: Upon request from the authors

Author contribution

728 VN, PC, BG, designed the research, VN, PC, RL and YW performed the research, VN and YW performed the model simulations and data analysis, and all authors wrote the paper. The authors have no conflict of interest to declare.

Acknowledgements

735 Funding was provided by the Laboratory for Sciences of Climate and Environment (LSCE), CEA, CNRS and UVSQ. RL acknowledges funding from the European Union's Horizon 2020 research and innovation program under grant agreement no.703813 for the Marie Skłodowska-Curie European Individual Fellowship "C-Leak". PC acknowledges support from the European Research Council Synergy grant ERC-2013-SyG-610028 IMBALANCE-P. [BG acknowledges support from the project ERANETMED2-72-209 ASSESS.](#) We also thank A.Chappell and D.S.Goll for their useful comments during the early stages of this research, and D.Zhu for helping out with the model simulations.

742 References

- Arneth, A., Sitch, S., Pongratz, J., Stocker, B. D., Ciais, P., Poulter, B., Bayer, A. D., Bondeau, A., Calle, L., Chini, L. P., Gasser, T., Fader, M., Friedlingstein, P., Kato, E., Li, W., Lindeskog, M., Nabel, J. E. M. S., Pugh, T. A. M., Robertson, E., Viovy, N., Yue, C. and Zaehle, S.: Historical carbon dioxide emissions caused by land-use changes are possibly larger than assumed, *Nat. Geosci.*, 10(January), doi:10.1038/NGEO2882, 2017.
- 749 Arora, V. K., Scinocca, J. F., Boer, G. J., Christian, J. R., Denman, K. L., Flato, G. M., Kharin, V. V., Lee, W. G. and Merryfield, W. J.: Carbon emission limits required to satisfy future representative concentration pathways of greenhouse gases, *Geophys. Res. Lett.*, 38, L05805, doi:10.1029/2010GL046270, 2011.
- Berhe, A. A., Harte, J., Harden, J. W. and Torn, M. S.: The Significance of the Erosion-induced Terrestrial Carbon Sink, *Bioscience*, 57(4), 337–346, 2007.
- [Billings, S. A., Buddemeier, R. W., DeB. Richter, D., Van Oost, K. and Bohling, G.: A simple method for estimating the influence of eroding soil profiles on atmospheric CO₂, *Global Biogeochem. Cycles*, 24\(2\), 1–14, doi:10.1029/2009GB003560, 2010.](#)
- 756 Bouchoms, S., Wang, Z., Vanacker, V., Doetterl, S. and Van Oost, K.: Modelling long-term soil organic carbon dynamics under the impact of land cover change and soil redistribution, *CATENA*, doi:10.1016/j.catena.2016.12.008, 2017.
- Chappell, A., Sanderman, J., Thomas, M. and Read, A.: The dynamics of soil redistribution and the implications for soil organic carbon accounting in agricultural south-eastern Australia, *Glob. Chang. Biol.*, 18, 2081–2088, doi:10.1111/j.1365-2486.2012.02682.x, 2012.
- 763 Chappell, A., Baldock, J. and Sanderman, J.: The global significance of omitting soil erosion from soil organic carbon cycling schemes, *Nat. Clim. Chang.*, (October), 1–5, doi:10.1038/NCLIMATE2829, 2015.
- Ciais, P., Sabine, C., Bala, G., Bopp, L., Brovkin, V., Canadell, J., Chhabra, A., DeFries, R., Galloway, J., Heimann,

Formatted: German (Germany)

- M., Jones, C., Quéré, C. Le, Myneni, R. B., Piao, S. and Thornton, P.: Carbon and Other Biogeochemical Cycles, in *Climate Change 2013: The physical science basis. Contribution of working group I to the fifth assessment report of the intergovernmental panel on climate change* [Stocker, T.F., D. Qin, G.-K. Plattner, M. Tignor, S.K. Allen, J. Boschung, A. Nauels, Y. Xia, pp. 465–570, Cambridge University Press, Cambridge, United Kingdom and New York, NY., 2013.
- 770 Doetterl, S., Van Oost, K. and Six, J.: Towards constraining the magnitude of global agricultural sediment and soil organic carbon fluxes, *Earth Surf. Process. Landforms*, doi:10.1002/esp.3198, 2012a.
- Doetterl, S., Van Oost, K. and Six, J.: Towards constraining the magnitude of global agricultural sediment and soil organic carbon fluxes, *Earth Surf. Process. Landforms*, 37(6), 642–655, doi:10.1002/esp.3198, 2012b.
- Frieler, K., Betts, R., Burke, E., Ciais, P., Denvil, S., Ebi, K., Eddy, T., Emanuel, K., Elliott, J., Galbraith, E., Simon, N., Halladay, K., Hattermann, F., Hickler, T., Hinkel, J., Mengel, M., Mouratiadou, I., Schmied, H. M., Vautard, R., Vliet, M. Van, Warszawski, L. and Zhao, F.: Assessing the impacts of 1.5 °C global warming – simulation protocol of the Inter-Sectoral Impact Model Intercomparison Project (ISIMIP2b), *Geosci. Model Dev. Discuss.*, (October), 1–59, doi:10.5194/gmd-2016-229, 2016.
- 777 Frieler, K., Lange, S., Piontek, F., Reyer, C. P. O., Schewe, J., Warszawski, L., Zhao, F., Chini, L., Denvil, S., Emanuel, K., Geiger, T., Halladay, K., Hurtt, G., Mengel, M., Murakami, D., Ostberg, S., Popp, A. and Riva, R.: Assessing the impacts of 1.5 °C global warming – simulation protocol of the Inter-Sectoral Impact Model Intercomparison Project (ISIMIP2b), *Geosci. Model Dev.*, 10, 4321–4345, 2017.
- Goll, D. S., Winkler, A. J., Raddatz, T., Dong, N., Colin Prentice, I., Ciais, P. and Brovkin, V.: Carbon-nitrogen interactions in idealized simulations with JSBACH (version 3.10), *Geosci. Model Dev.*, 10(5), 2009–2030, doi:10.5194/gmd-10-2009-2017, 2017.
- 784 Guenet, B., Moyano, F. E., Peylin, P., Ciais, P. and Janssens, I. A.: Towards a representation of priming on soil carbon decomposition in the global land biosphere model ORCHIDEE (version 1.9.5.2), *Geosci. Model Dev.*, 9, 841–855, doi:10.5194/gmd-9-841-2016, 2016.
- Guimberteau, M., Zhu, D., Maignan, F., Huang, Y., Yue, C., Dantec-N?d?lec, S., Ottl?, C., Jornet-Puig, A., Bastos, A., Laurent, P., Goll, D., Bowring, S., Chang, J., Guenet, B., Tifafi, M., Peng, S., Krinner, G., Ducharne, A., Wang, F., Wang, T., Wang, X., Wang, Y., Yin, Z., Lauerwald, R., Joetzjer, E., Qiu, C., Kim, H. and Ciais, P.: ORCHIDEE-MICT (revision 4126), a land surface model for the high-latitudes: model description and validation, *Geosci. Model Dev. Discuss.*, (revision 4126), 1–65, doi:10.5194/gmd-2017-122, 2017.
- 791 Harden, J. W., Sharpe, J. M., Parton, W. J., Ojima, D. S., Fries, T. L., Huntington, T. G. and Dabney, S. M.: Dynamic replacement and loss of soil carbon on eroding cropland, *Global Biogeochem. Cycles*, 13(4), 885–901, doi:10.1029/1999GB900061, 1999.
- Hay R.K.M.: Harvest index: a review of its use in plant breeding and crop physiology, *Ann. appl. Biol.*, 126, 197–216, 1995.
- 798 Hempel, S., Frieler, K., Warszawski, L., Schewe, J. and Piontek, F.: A trend-preserving bias correction – the ISIMIP approach, *Earth Syst. Dyn.*, 4, 219–236, doi:10.5194/esd-4-219-2013, 2013.
- Hengl, T., De Jesus, J. M., MacMillan, R. A., Batjes, N. H., Heuvelink, G. B. M., Ribeiro, E., Samuel-Rosa, A.,

- Kempen, B., Leenaars, J. G. B., Walsh, M. G. and Gonzalez, M. R.: SoilGrids1km - Global soil information based on automated mapping, *PLoS One*, 9(8), doi:10.1371/journal.pone.0105992, 2014.
- 805 Hilton, R. G., Galy, A., Hovius, N., Chen, M., Hornig, M. and Chen, H.: Tropical-cyclone-driven erosion of the terrestrial biosphere from mountains, *Nat. Geosci. Lett.*, 1, 759, doi:10.1038/ngeo333, 2008.
- Hilton, R. G., Meunier, P., Hovius, N., Bellingham, P. J. and Galy, A.: Landslide impact on organic carbon cycling in a temperate montane forest, *Earth Surf. Process. Landforms*, 1679(July), 1670–1679, doi:10.1002/esp.2191, 2011.
- Hoffmann, T., Schlummer, M., Notebaert, B., Verstraeten, G. and Korup, O.: Carbon burial in soil sediments from Holocene agricultural erosion, Central Europe, *Global Biogeochem. Cycles*, 27(3), 828–835, doi:10.1002/gbc.20071, 2013a.
- 812 Hoffmann, T., Mudd, S. M., van Oost, K., Verstraeten, G., Erkens, G., Lang, a., Middelkoop, H., Boyle, J., Kaplan, J. O., Willenbring, J. and Aalto, R.: Short Communication: Humans and the missing C-sink: erosion and burial of soil carbon through time, *Earth Surf. Dyn.*, 1(1), 45–52, doi:10.5194/esurf-1-45-2013, 2013b.
- Houghton, R. A.: Revised estimates of the annual net flux of carbon to the atmosphere from changes in land use and land management 1850-2000, *Tellus, Ser. B Chem. Phys. Meteorol.*, 55(2), 378–390, doi:10.1034/j.1600-0889.2003.01450.x, 2003.
- Houghton, R. A. and Nassikas, A. A.: Global and regional fluxes of carbon from land use and land cover change 1850–2015, *Global Biogeochem. Cycles*, 31(3), 456–472, doi:10.1002/2016GB005546, 2017.
- 819 Houghton, R. A., Hackler, J. L. and Lawrence, K. T.: The U . S . Carbon Budget : Contributions from Land-Use Change, *Science* (80-), 285(July), 574–579, 1999.
- Ito, A.: Simulated impacts of climate and land-cover change on soil erosion and implication for the carbon cycle, 1901 to 2100, *Geophys. Res. Lett.*, 34(9), n/a-n/a, doi:10.1029/2007GL029342, 2007.
- Khatiwala, S., Primeau, F. and Hall, T.: Reconstruction of the history of anthropogenic CO₂ concentrations in the ocean, *Nature*, 462(7271), 346–349, doi:10.1038/nature08526, 2009.
- 826 Krinner, G., Viovy, N., de Noblet-Ducoudré, N., Ogée, J., Polcher, J., Friedlingstein, P., Ciais, P., Sitch, S. and Prentice, I. C.: A dynamic global vegetation model for studies of the coupled atmosphere-biosphere system, *Global Biogeochem. Cycles*, 19(1), 1–33, doi:10.1029/2003GB002199, 2005.
- Lal, R.: Soil erosion and the global carbon budget., *Environ. Int.*, 29(4), 437–50, doi:10.1016/S0160-4120(02)00192-7, 2003.
- Lauerwald, R., Regnier, P., Camino-Serrano, M., Guenet, B., Guimberteau, M., Ducharme, A., Polcher, J. and Ciais, P.: ORCHILEAK: A new model branch to simulate carbon transfers along the terrestrial-aquatic continuum of the Amazon basin, *Geosci. Model Dev. Discuss.*, (April), doi:10.5194/gmd-2017-79, 2017.
- 833 Li, W., Ciais, P., Peng, S., Yue, C., Wang, Y., Thurner, M., Sassan, S., Arneth, A., Avitabile, V., Carvalhais, N., Harper, A. B., Kato, E., Koven, C., Liu, Y. Y., Nabel, J. E. M. S., Pan, Y., Pongratz, J., Poulter, B., Pugh, T. A. M., Santoro, M., Sitch, S., Stocker, B. D. and Viovy, N.: Land-use and land-cover change carbon emissions between 1901 and 2012 constrained by biomass observations, *Biogeosciences Discuss.*, (June), doi:10.5194/bg-2017-186, 2017.
- Lugato, E., Paustian, K., Panagos, P., Jones, A. and Borrelli, P.: Quantifying the erosion effect on current carbon

- budget of European agricultural soils at high spatial resolution, *Glob. Chang. Biol.*, doi:10.1111/gcb.13198, 2016.
- 840 Mehran A., AghaKouchak A., and P. T. J.: Evaluation of CMIP5 continental precipitation simulations relative to satellite-based gauge-adjusted observations, *J. Geophys. Res. Atmos.*, (119), 1695–1707, doi:10.1002/2013JD021152. Received, 2014.
- Montgomery, D. R.: Soil erosion and agricultural sustainability, , 104(33), 13268–13272, 2007.
- Nadeu, E., Gobin, A., Fiener, P., van Wesemael, B. and van Oost, K.: Modelling the impact of agricultural management on soil carbon stocks at the regional scale: the role of lateral fluxes., *Glob. Chang. Biol.*, 21(8), 3181–92, doi:10.1111/gcb.12889, 2015.
- 847 Naipal, V., Reick, C., Pongratz, J. and Van Oost, K.: Improving the global applicability of the RUSLE model - Adjustment of the topographical and rainfall erosivity factors, *Geosci. Model Dev.*, 8(9), doi:10.5194/gmd-8-2893-2015, 2015.
- Naipal, V., Reick, C., Van Oost, K., Hoffmann, T. and Pongratz, J.: Modeling long-term, large-scale sediment storage using a simple sediment budget approach, *Earth Surf. Dyn.*, 4(2), doi:10.5194/esurf-4-407-2016, 2016.
- Van Oost, K., Quine, T. a, Govers, G., De Gryze, S., Six, J., Harden, J. W., Ritchie, J. C., McCarty, G. W., Heckrath, G., Kosmas, C., Giraldez, J. V, da Silva, J. R. M. and Merckx, R.: The impact of agricultural soil erosion on the global carbon cycle., *Science*, 318(5850), 626–9, doi:10.1126/science.1145724, 2007.
- 854 Van Oost, K., Verstraeten, G., Doetterl, S., Notebaert, B., Wiaux, F. and Broothaerts, N.: Legacy of human-induced C erosion and burial on soil – atmosphere C exchange, *PNAS*, 109(47), 19492–19497, doi:10.1073/pnas.1211162109/-/DCSupplemental.www.pnas.org/cgi/doi/10.1073/pnas.1211162109, 2012.
- Peel, M. C., Finlayson, B. L. and McMahon, T. A.: Updated world map of the Koeppen-Geiger climate classification, *Hydrol. Earth Syst. Sci.*, 11, 1633–1644, 2007.
- Peng, S., Ciais, P., Maignan, F., Li, W., Chang, J., Wang, T. and Yue, C.: Sensitivity of land use change emission estimates to historical land use and land cover mapping, *Global Biogeochem. Cycles*, 31(4), 626–643, doi:10.1002/2015GB005360, 2017.
- 861 Piao, S., Ciais, P., Friedlingstein, P., De Noblet-Ducoudré, N., Cadule, P., Viovy, N. and Wang, T.: Spatiotemporal patterns of terrestrial carbon cycle during the 20th century, *Global Biogeochem. Cycles*, 23(4), 1–16, doi:10.1029/2008GB003339, 2009.
- Le Quéré, C., Andrew, R. M., Canadell, J. G., Sitch, S., Ivar Korsbakken, J., Peters, G. P., Manning, A. C., Boden, T. A., Tans, P. P., Houghton, R. A., Keeling, R. F., Alin, S., Andrews, O. D., Anthoni, P., Barbero, L., Bopp, L., Chevallier, F., Chini, L. P., Ciais, P., Currie, K., Delire, C., Doney, S. C., Friedlingstein, P., Gkritzalis, T., Harris, I., Hauck, J., Haverd, V., Hoppema, M., Klein Goldewijk, K., Jain, A. K., Kato, E., Körtzinger, A., Landschützer, P., Lefèvre, N., Lenton, A., Lienert, S., Lombardozzi, D., Melton, J. R., Metzl, N., Millero, F., Monteiro, P. M. S., Munro, D. R., Nabel, J. E. M. S., Nakaoka, S. I., O’Brien, K., Olsen, A., Omar, A. M., Ono, T., Pierrot, D., Poulter, B., Rödenbeck, C., Salisbury, J., Schuster, U., Schwinger, J., Séférian, R., Skjelvan, I., Stocker, B. D., Sutton, A. J., Takahashi, T., Tian, H., Tilbrook, B., Van Der Laan-Luijckx, I. T., Van Der Werf, G. R., Viovy, N., Walker, A. P., Wiltshire, A. J. and Zaehle, S.: Global Carbon Budget 2016, *Earth Syst. Sci. Data*, 8(2), 605–649, doi:10.5194/essd-8-605-2016, 2016.
- 875

- Quinton, J. N., Govers, G., Van Oost, K. and Bardgett, R. D.: The impact of agricultural soil erosion on biogeochemical cycling, *Nat. Geosci.*, 3(5), 311–314, doi:10.1038/ngeo838, 2010.
- Regnier, P., Friedlingstein, P., Ciais, P., Mackenzie, F. T., Gruber, N., Janssens, I. a., Laruelle, G. G., Lauerwald, R., Luysaert, S., Andersson, A. J., Arndt, S., Arnosti, C., Borges, A. V., Dale, A. W., Gallego-Sala, A., Godd ris, Y., Goossens, N., Hartmann, J., Heinze, C., Ilyina, T., Joos, F., LaRowe, D. E., Leifeld, J., Meysman, F. J. R., Munhoven, G., Raymond, P. a., Spahni, R., Suntharalingam, P. and Thullner, M.: Anthropogenic perturbation of the carbon fluxes from land to ocean, *Nat. Geosci.*, 6(8), 597–607, doi:10.1038/ngeo1830, 2013.
- 882 Scharlemann, J. P. W., Tanner, E. V. J., Hiederer, R. and Kapos, V.: Global soil carbon: Understanding and managing the largest terrestrial carbon pool, *Carbon Manag.*, 5(1), 81–91, doi:10.4155/cmt.13.77, 2014.
- Shangguan H.W., Dai Y., Duan Q., Liu B., Y. H.: A global soil data set for earth system modeling Wei, J. *Adv. Model. Earth Syst.*, 6, 249–263, doi:10.1002/2013MS000293.Received, 2014.
- Stallard, R. F.: Terrestrial sedimentation and the carbon cycle : Coupling weathering and erosion to carbon burial, *Global Biogeochem. Cycles*, 12(2), 231–257, 1998.
- 889 Stocker, B. D., Feissli, F., Strassmann, K. M. and Spahni, R.: Past and future carbon fluxes from land use change, shifting cultivation and wood harvest, *Tellus B Chem. Phys. Meteorol.*, 66, 23188, doi:10.3402/tellusb.v66.23188, 2014.
- Taylor, K. E., Stouffer, R. J. and Meehl, G. A.: A Summary of the CMIP5 Experiment Design, *Am. Meteorol. Soc.*, 93, 485–498, doi:https://doi.org/10.1175/BAMS-D-11-00094.1, 2012.
- Thonicke, K., Spessa, A., Prentice, I. C., Harrison, S. P. and Dong, L.: The influence of vegetation , fire spread and fire behaviour on biomass burning and trace gas emissions : results from a process-based model, *Biogeosciences*, 7, 1991–2011, doi:10.5194/bg-7-1991-2010, 2010.
- 896 Tifafi, M., Guenet, B. and Hatt , C.: Large Differences in Global and Regional Total Soil Carbon Stock Estimates Based on SoilGrids, HWSD, and NCSCD: Intercomparison and Evaluation Based on Field Data From USA, England, Wales, and France, *Global Biogeochem. Cycles*, 32(1), 42–56, doi:10.1002/2017GB005678, 2018.
- Todd-Brown, K. E. O., Randerson, J. T., Hopkins, F., Arora, V., Hajima, T., Jones, C., Shevliakova, E., Tjiputra, J., Volodin, E., Wu, T., Zhang, Q. and Allison, S. D.: Changes in soil organic carbon storage predicted by Earth system models during the 21st century, *Biogeosciences*, 11(8), 2341–2356, doi:10.5194/bg-11-2341-2014, 2014.
- 903 Valentin, C., Poesen, J. and Li, Y.: Gully erosion : Impacts , factors and control, *CATENA*, 63, 132–153, doi:10.1016/j.catena.2005.06.001, 2005.
- Wang, Z., Doetterl, S., Vanclooster, M., van Wesemael, B. and Van Oost, K.: Constraining a coupled erosion and soil organic carbon model using hillslope-scale patterns of carbon stocks and pool composition, *J. Geophys. Res. Biogeosciences*, 120, doi:10.1002/2014JG002768, 2015a.
- Wang, Z., Van Oost, K. and Govers, G.: Predicting the long-term fate of buried organic carbon in colluvial soils, *Global Biogeochem. Cycles*, doi:10.1002/2014GB004912, 2015b.
- 910 Wang, Z., Hoffmann, T., Six, J., Kaplan, J. O., Govers, G., Doetterl, S. and Van Oost, K.: Human-induced erosion has offset one-third of carbon emissions from land cover change, *Nat. Clim. Chang.*, 7(5), 345–349, doi:10.1038/nclimate3263, 2017.

Worrall F., Burt T.P., H. N. J. K.: The fluvial flux of particulate organic matter from the UK: the emission factor of soil erosion, *Earth Surf. Process. Landforms*, 41(1), 61–71, 2016.

Yue, C., Ciais, P., Luyssaert, S., Li, W., Mcgrath, M. J., Chang, J. F., Peng, S. S. and Amsterdam, V. U.: Representing anthropogenic gross land use change, wood harvest and forest age dynamics in a global vegetation model ORCHIDEE-MICT (r4259), *Geosci. Model Dev. Discuss. Model Dev. Discuss.*, 2017.

917 Yue, Y., Ni, J., Ciais, P., Piao, S., Wang, T., Huang, M., Borthwick, A. G. L., Li, T., Wang, Y., Chappell, A. and Van Oost, K.: Lateral transport of soil carbon and land-atmosphere CO₂ flux induced by water erosion in China, *PNAS*, 113(24), 6617–6622, doi:10.1073/pnas.1523358113, 2016.

Zhang, H., Liu, S., Yuan, W., Dong, W., Ye, A., Xie, X., Chen, Y., Liu, D., Cai, W. and Mao, Y.: Inclusion of soil carbon lateral movement alters terrestrial carbon budget in China, *Sci. Rep.*, 4(7247), doi:10.1038/srep07247, 2014.

924 Zhao, J., Van Oost, K., Chen, L. and Govers, G.: Moderate topsoil erosion rates constrain the magnitude of the erosion-induced carbon sink and agricultural productivity losses on the Chinese Loess Plateau, *Biogeosciences Discuss.*, 12(17), 14981–15010, doi:10.5194/bgd-12-14981-2015, 2015.

Zhu, D., Peng, S., Ciais, P., Zech, R., Krinner, G., Zimov, S. and Grosse, G.: Simulating soil organic carbon in yedoma deposits during the Last Glacial Maximum in a land surface model, *Geophys. Res. Lett.*, 43(10), 5133–5142, doi:10.1002/2016GL068874, 2016.

931 Table 1: Description of simulations used in this study. The S1 simulation is also the control simulation (CTR). [S1](#) and [S2 minimum and maximum](#) are the sensitivity simulations using minimum or maximum soil erosion rates. “Best” stands for the best estimated soil erosion rates using optimal values for the R and C factors of the [Adj.RUSLE model](#).

Simulation	Climate change	CO ₂ change	Land use change	Erosion
S1	Yes	Yes	Yes	Best Yes
S1 minimum	Yes	Yes	Yes	Minimum
S1 maximum	Yes	Yes	Yes	Maximum
S2	Yes	Yes	No	Best Yes
S2 minimum	Yes	Yes	No	Minimum
S2 maximum	Yes	Yes	No	Maximum
S1-S2	No	Yes	Yes	Best Yes
S3	Yes	Yes	Yes	No
S4	Yes	Yes	No	No
S3-S4	No	Yes	Yes	No
S5	Yes	No	Yes	Best Yes
S6	Yes	No	No	Best Yes

S5-S6	No	No	Yes	Best Yes
S7	Yes	No	Yes	No
S8	Yes	No	No	No
S7-S8	No	No	Yes	No

Table 2: Area weighted average and standard deviation of soil and SOC erosion rates per PFT for the year 2005AD;

[the uncertainty range for soil erosion rates is 25 - 53 % and for SOC erosion rates 16-50%. For more details on the uncertainty ranges see table.. of the supporting material.](#) ~~the low standard deviation for SOC erosion is due to the coarse resolution of the emulator~~

PFT	Mean soil erosion (t ha ⁻¹ y ⁻¹)	Standard deviation soil erosion (t ha ⁻¹ y ⁻¹)	Mean SOC erosion (kg C ha ⁻¹ y ⁻¹)	Standard deviation SOC erosion (kg C ha ⁻¹ y ⁻¹)
Crop	2.45 1.71	35 24.95	10.384	466 0.99
Grass	1.808	30 32.67	5.79 29	91 3.7
Forest	0.34 26	32 31	1.34 6.7	140 7

938 Table 3: Model estimates per continent of area-weighted average annual soil erosion and SOC erosion rates for the

year 2005, their spatial standard deviations, and the changes in average soil and SOC erosion rates since 1851; [the uncertainty range for soil and SOC erosion rates is 2 - 36 % and 3-52%, respectively. The uncertainty range for the changes in soil and SOC erosion rates since 1851 is 3 – 83 % and 11-166%, respectively. For more details on the uncertainty ranges see table.. of the supporting material.](#) ~~the low standard deviation for SOC erosion is due to the coarse resolution of the emulator.~~

Region	Mean soil erosion rate	Standard deviation soil erosion rate	Change in mean soil erosion rate	Mean SOC erosion rate	Standard deviation SOC erosion rate	Change in mean SOC erosion rate
	2005	2005	2005 -1851	2005	2005	2005-1851
	(t ha ⁻¹ y ⁻¹)	(t ha ⁻¹ y ⁻¹)	(t ha ⁻¹ y ⁻¹)	(kg C ha ⁻¹ y ⁻¹)	(kg C ha ⁻¹ y ⁻¹)	(kg C ha ⁻¹ y ⁻¹)
Africa	2.35 2.69	59.96 68.47	0.58 0.69	13.19 21	95.22 22	4.31 7.3
Asia	5.66 6.03	157.90 167.83	0.21 0.23	58.03 75	802.53 12	3.23 5
Europe	2.07 2.45	62.50 73.70	0.39 0.48	16.68 21	338.03 5	1.39 2.1
Australia	1.40 1.46	16.29 16.98	-0.47 -0.50	5.16 5	22.91 0.2	1.82 -0.6
South-America	4.52 4.69	113.26 117.58	1.29 1.35	74.42 86	1515.04 18	38.97 38.4
North-	2.60 2.83	58.62 63.68	0.13 0.15	32.88 45	556.44 9	3.14 4.4

America						
Global	<u>3.613-92</u>	<u>96.43104.48</u>	<u>0.450-50</u>	<u>38.5650</u>	<u>666.399-5</u>	<u>8.9410.6</u>

Table 4: Model estimates per continent of changes in SOC stocks since 1851 from simulations S1, S2, S1-S2, S3,

945 S4, S3-S4. [Details on the uncertainty due to soil erosion in the SOC stock changes of simulations S1 and S2 can be found in table ... of the supporting material.](#)

Region	Change SOC stocks S1	Change SOC stocks S2	Change SOC stocks S1-S2	Change SOC stocks S3	Change SOC stocks S4	Change SOC stocks S3-S4
	Pg C	Pg C	Pg C	Pg C	Pg C	Pg C
Africa	<u>-1.550-91</u>	<u>-0.243-11</u>	<u>-1.31-2-2</u>	<u>-1.541-35</u>	<u>-0.552-79</u>	<u>-0.98-1-44</u>
Asia	<u>-0.36-2-53</u>	<u>7.9412-74</u>	<u>-8.31-15-27</u>	<u>0.65-0-29</u>	<u>7.1111-08</u>	<u>-6.47-11-37</u>
Europe	<u>-3.33-2-68</u>	<u>1.782-98</u>	<u>-5.12-5-66</u>	<u>-4.35-3-38</u>	<u>1.523-08</u>	<u>-5.87-6-46</u>
Australia	<u>0.210-09</u>	<u>0.050-66</u>	<u>0.16-0-57</u>	<u>0.290-24</u>	<u>0.010-66</u>	<u>0.28-0-42</u>
South-America	<u>2.24-0-91</u>	<u>2.825-9</u>	<u>-0.59-6-81</u>	<u>3.750-48</u>	<u>2.064-86</u>	<u>1.69-4-38</u>
North-America	<u>-2.62-4-84</u>	<u>3.195-11</u>	<u>-5.81-9-95</u>	<u>-2.5-4-18</u>	<u>3.035-1</u>	<u>-5.53-9-28</u>
Global	<u>-5.35-9-96</u>	<u>15.9330-5</u>	<u>-21.29-40-46</u>	<u>-3.3-5-78</u>	<u>13.8627-57</u>	<u>-17.16-33-35</u>

Table 5: Statistics of a grid cell by grid cell comparison of global SOC stocks between GSDE soil database and simulations S1 (with erosion) and S3 (without erosion). RMSE is the root mean square error and r-value is the correlation coefficient of the linear regression between GSDE and S1 of S3.

Soil depth (m)	GSDE SOC total (Pg)	S1 SOC total (Pg)	S3 SOC total (Pg)	RMSE S1	RMSE S3	r-value S1	r-value S3
0.3	670	<u>428742</u>	<u>5561058</u>	<u>521878.07</u>	<u>5861101.62</u>	<u>0.430-53</u>	<u>0.440-57</u>
1	1356	<u>6721247</u>	<u>8461677</u>	<u>14077126.39</u>	<u>10213155.63</u>	<u>0.520-59</u>	<u>0.510-58</u>
2	1748	<u>10011936</u>	<u>12842589</u>	<u>12968211.76</u>	<u>13195267.45</u>	<u>0.560-58</u>	<u>0.550-57</u>

Table 6: Comparison of our model estimates of agricultural soil and SOC loss fluxes for the year 2005 with high-resolution model/observation estimates. *Quinton et al. (2010) included also pasture land in their study.

Study	Soil loss Pg y ⁻¹	SOC loss Pg C y ⁻¹
Van Oost et al. (2007)	17	0.25
Doetterl et al. (2012)	13	0.24
*Quinton et al. (2010)	28	0.5±0.15

Chappell et al. (2015)	17- 65	0.37 – 1.27
Wang et al. (2017)	17.7±1.70	0.44±0.06
This study	<u>12.28+4.624</u>	<u>0.16+0.069</u>

952 | Table 7: Comparison of our model [best](#) estimates of agricultural soil erosion and SOC erosion rates for the year 2005 with [best](#) model/observation estimates from Doetterl et al. (2012) per continent. [The uncertainty range for the present-day sediment and SOC fluxes is 18 – 62 % and 5-51%, respectively. The uncertainty range in the values of Doetterl et al. \(2012\) is 30 - 70%.](#)

Region	<i>Our Study</i>		<i>Doetterl et al. (2012)</i>	
	Sediment flux 2005 Pg y ⁻¹	SOC flux 2005 Tg C y ⁻¹	Sediment flux 2000 Pg y ⁻¹	SOC flux 2000 Tg C y ⁻¹
Africa	2.6	<u>209.30</u>	2.4	39.5
Asia	5.4	<u>5474.30</u>	4.9	90.0
Europe	2.1	<u>306.85</u>	1.9	39.5
Australia	0.2	<u>2.543</u>	0.3	4.3
South- America	1.6	<u>397.05</u>	1.4	26.7
North- America	0.7	<u>127.40</u>	1.6	31.5
Total	<u>12.36</u>	<u>16192.52</u>	12.5	231.5

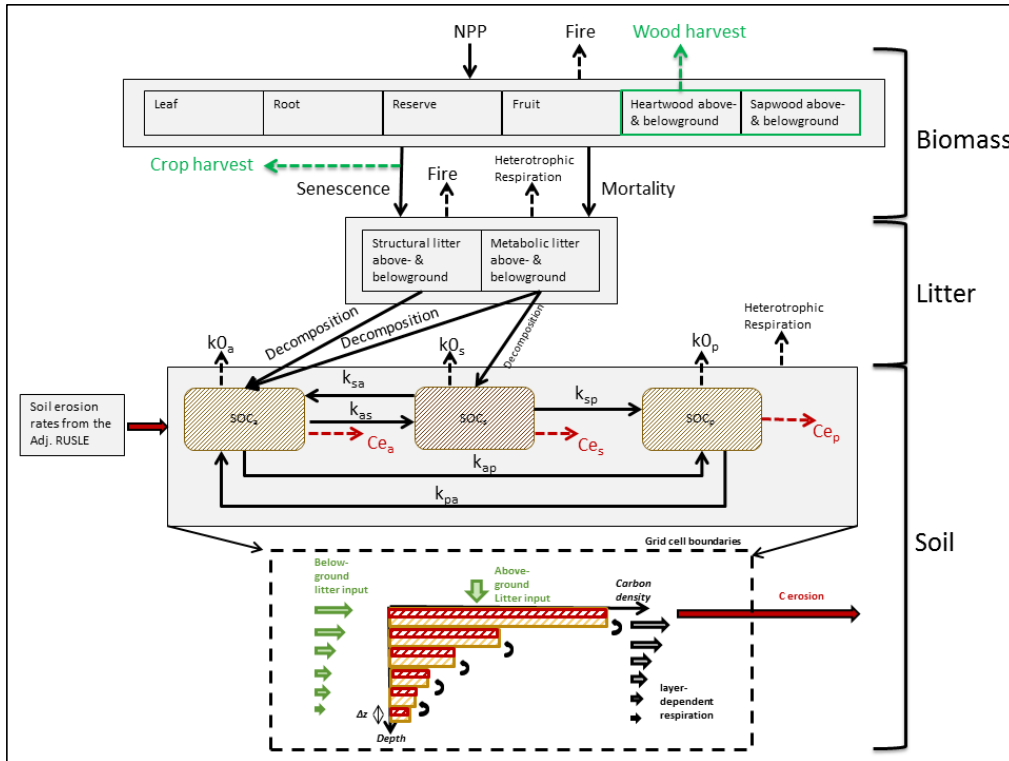
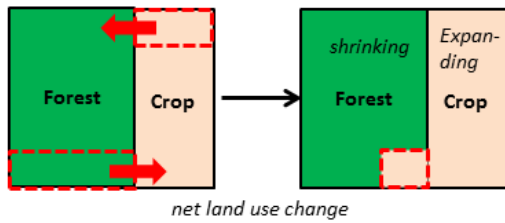
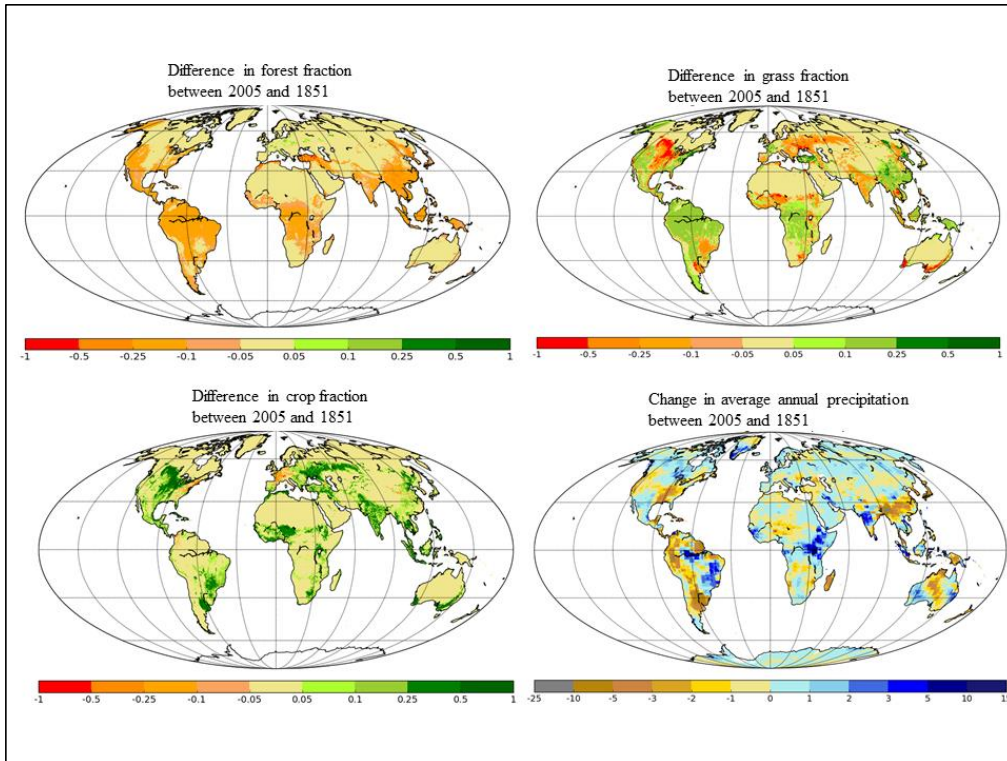


Figure 1(A): The structure of the C emulator (see variable names in the text, paragraph 2.3). The C erosion fluxes are represented by the red arrows and calculated using the soil erosion rates from the Adj.RUSLE model



1. Read PFT fractions
2. Identify expanding & shrinking PFT's
3. Collect wood products (wood harvest)
4. Sum the biomass of the area lost of all shrinking PFT's
5. Allocate this to the metabolic/structural litter of expanding PFT's
6. Sum the litter of the area lost of all shrinking PFT's
7. Allocate this to the expanding PFT's
8. Distribute biomass and litter over new PFT area
9. Sum the SOC per soil layer of the area lost of all shrinking PFT's
10. Allocate this to the respective soil layer of the expanding PFT's; In this way the SOC soil profile of the expanding and shrinking PFTs gets mixed
11. Distribute SOC over new PFT area

Figure 1(B): The land use change module of the emulator



959 Figure 2: Spatial patterns of the difference in forest, crop and grassland area between 1851 and 2005 represented as a fraction of a grid cell. And spatial patterns of the change in average annual precipitation between 1851 and 2005 in mm y^{-1} , calculated as the total change in precipitation over the period 1851 – 2005 and divided by the number of years in this period.

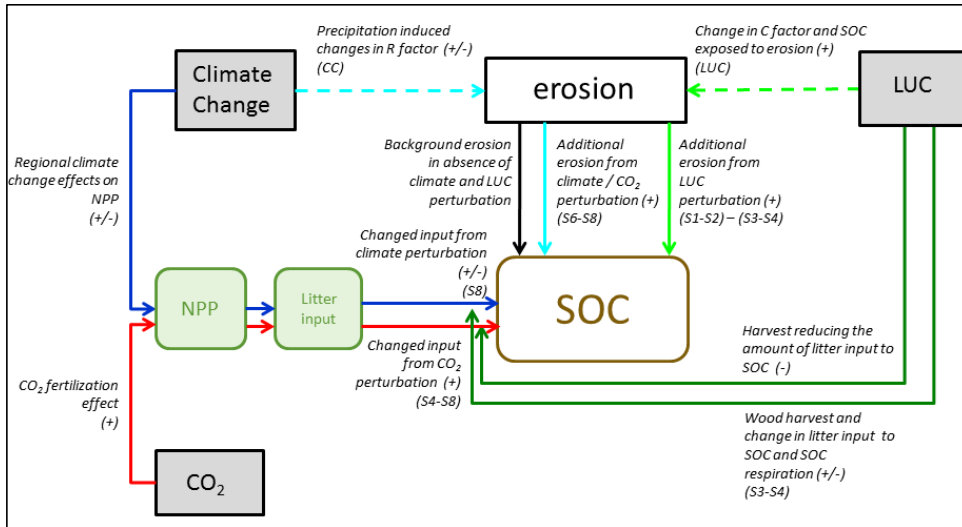


Figure 3: Conceptual diagram of SOC affected by erosion in presence of other perturbations of the carbon cycle, namely climate variability, increasing atmospheric CO₂ concentrations and land use change. A separation of these components and of the role of erosion is obtained with the factorial simulations (S1-S8), presented in Table 1

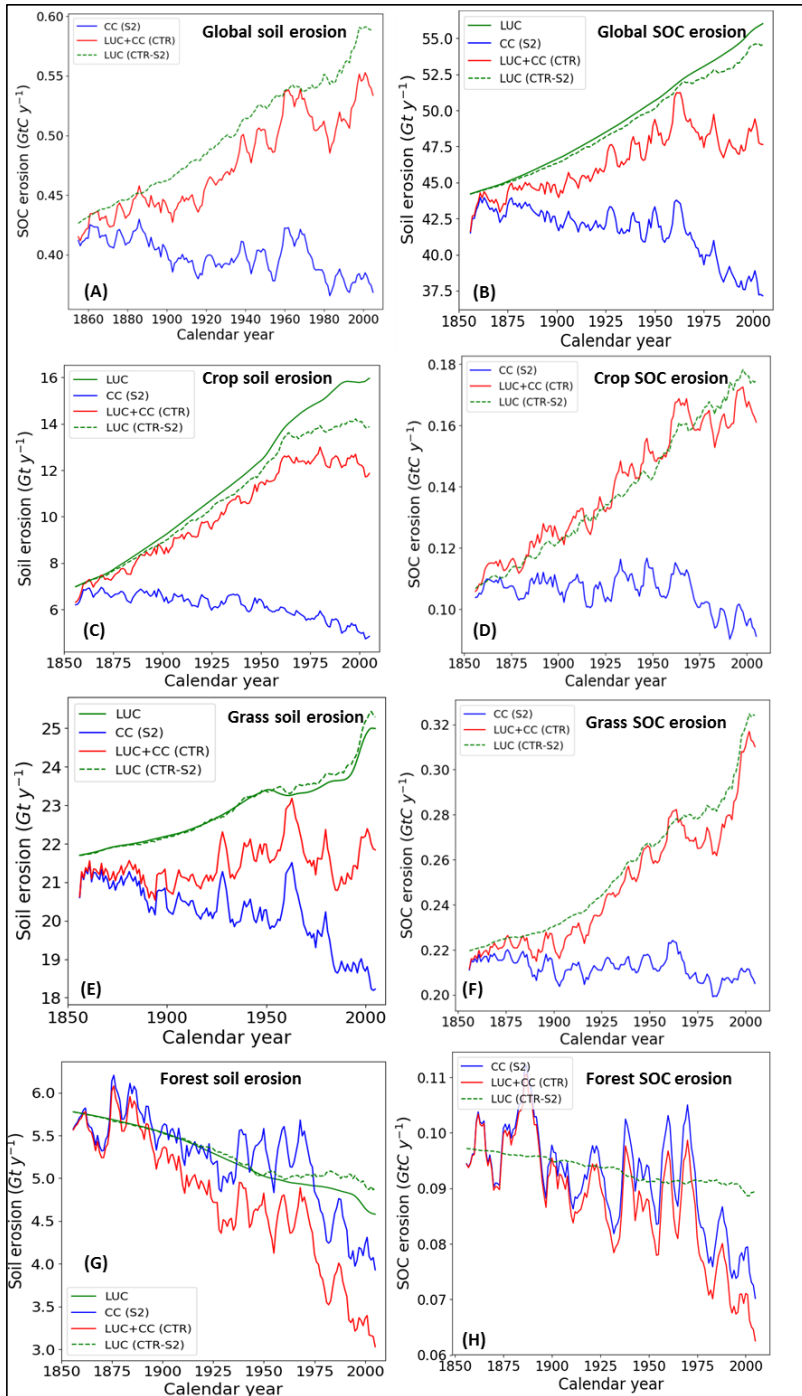
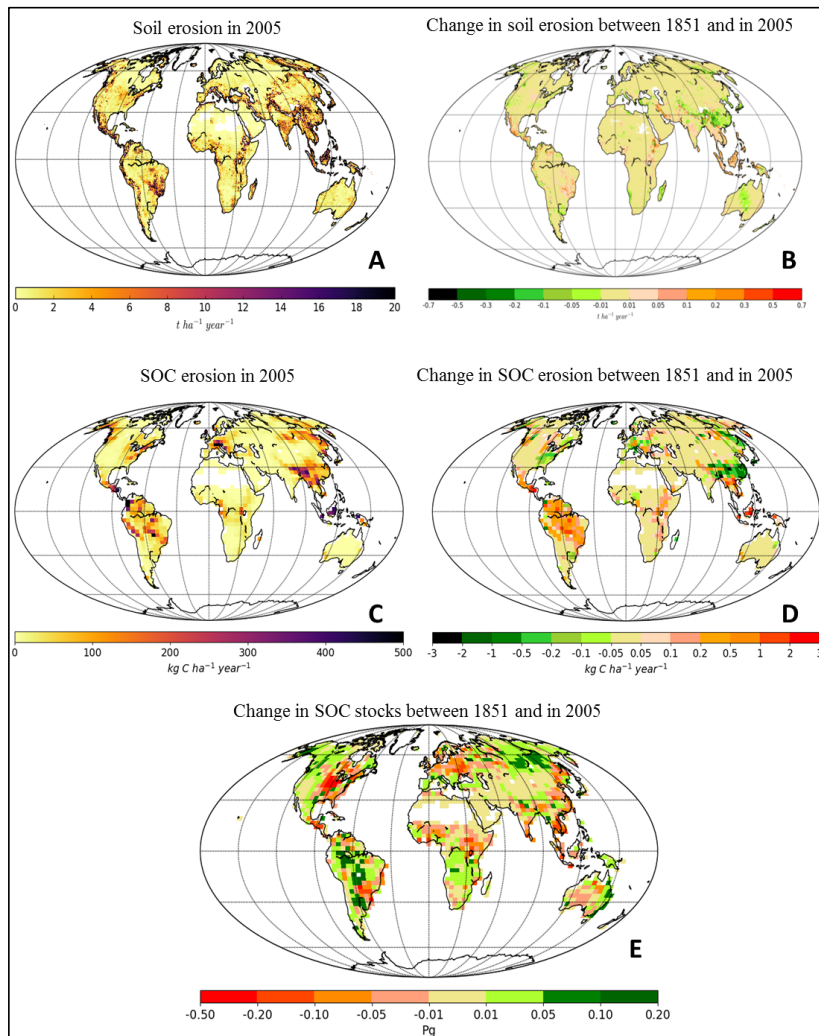


Figure 4: (A) Global annual soil erosion rates, (B) global annual SOC erosion rates, (C) agricultural annual soil erosion rates, (D) agricultural annual SOC erosion rates, (E) grassland annual soil erosion rates, (F) grassland annual SOC erosion rates, (G) forest annual soil erosion rates and (H) forest annual SOC erosion rates over the period 1850-2005 for scenario's with only LUC (green lines), scenario with only climate and CO₂ change (blue line) and scenario with LUC, climate and CO₂ change (red line). In figures A, C, E, and G the dashed green line is the difference between the CTR and S2 simulations, while the straight green line is the LUC-only simulation with the Adj.RUSLE model.



Comment [VN19]: No significant differences to figures 4-9 due to changes in the vertical discretization scheme

Comment [VN20]:

Reviewer #1: "Figure 4. I do not fully understand why climate change either decrease or not change erosion?"

Answer: With climate change we mean temperature and precipitation changes. For soil erosion only precipitation changes are of interest. Globally we find that average yearly precipitation shows a slightly decreasing trend over the period 1950 – 2005 according to the ISIMIP2b dataset used to calculate soil erosion rates. A global smaller total precipitation with respect to 1850 AD will lead to smaller soil erosion rates when LUC is not included. The decrease in total precipitation over land is mostly coming from the tropics, where due to large precipitation amounts a change in precipitation can alter soil erosion significantly. At the same time precipitation is very variable and might not lead to a significant global net change in soil erosion rates over the total period 1850-2005. This result might be contradictory to the fact that major soil erosion events are caused by storms. But in our case we model only rill and interrill erosion, which is usually a slow process and previous studies have shown that land use change is usually the main driver of behind accelerated rates of this type of soil erosion. Furthermore, there are very few studies that have quantified the individual effects of precipitation change versus land use change on soil erosion rates over a sufficiently long time period. Therefore, it is difficult to verify this result. However, our soil erosion model performs well for present-day and therefore any possible biases here could be mainly related to biases in precipitation rates, and soil parameters. We agree that this is an interesting point raised by the reviewer and added some additional sentences explaining the trend in beginning of chapter 4.2.

Fig 5: (A) Average annual soil erosion rates at a 5 arcmin resolution in the year 2005, (B) change in average annual soil erosion rates over the period 2005-1850, (C) average annual SOC erosion rates at a resolution of 2.5x3.75 degrees in 2005, (D) change in average annual SOC erosion rates over the period 2005-1850, and (E) difference in SOC stocks at a resolution of 2.5x3.75 degrees between the year 2005 and 1850 (CTR simulation). For the SOC stocks positive values (green color) indicate a gain, while negative values (red color) indicating a loss. For the erosion rates positive values (red color) indicate an increase over 1850 - 2005, while negative values (green color) indicate a decrease over 1850 - 2005

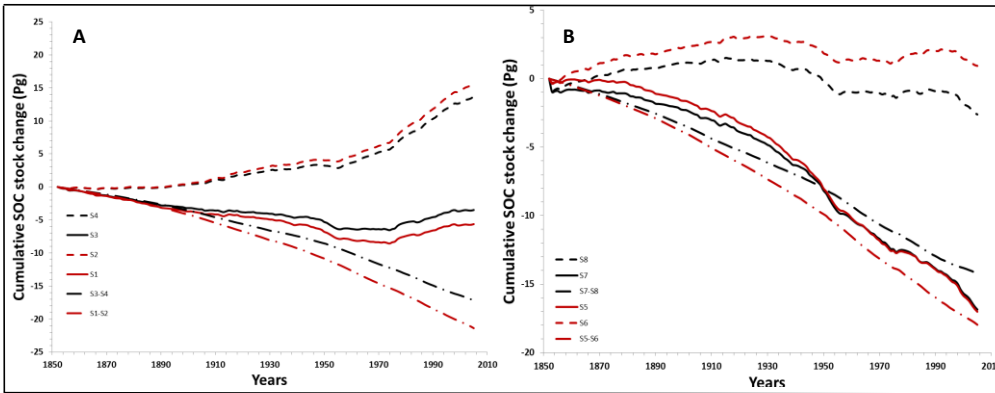
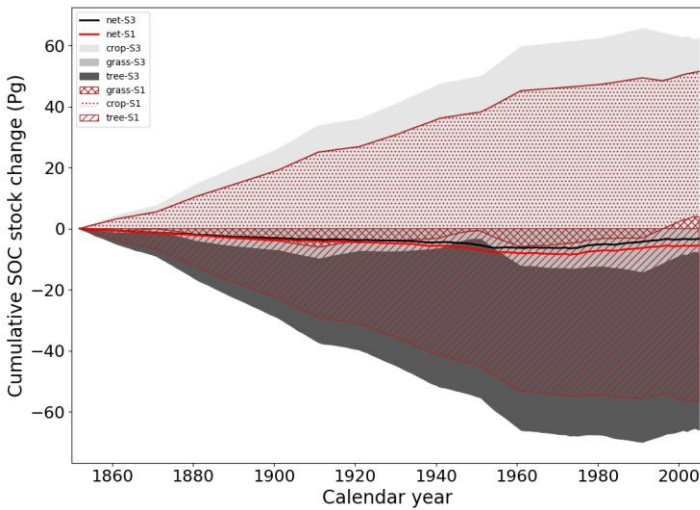
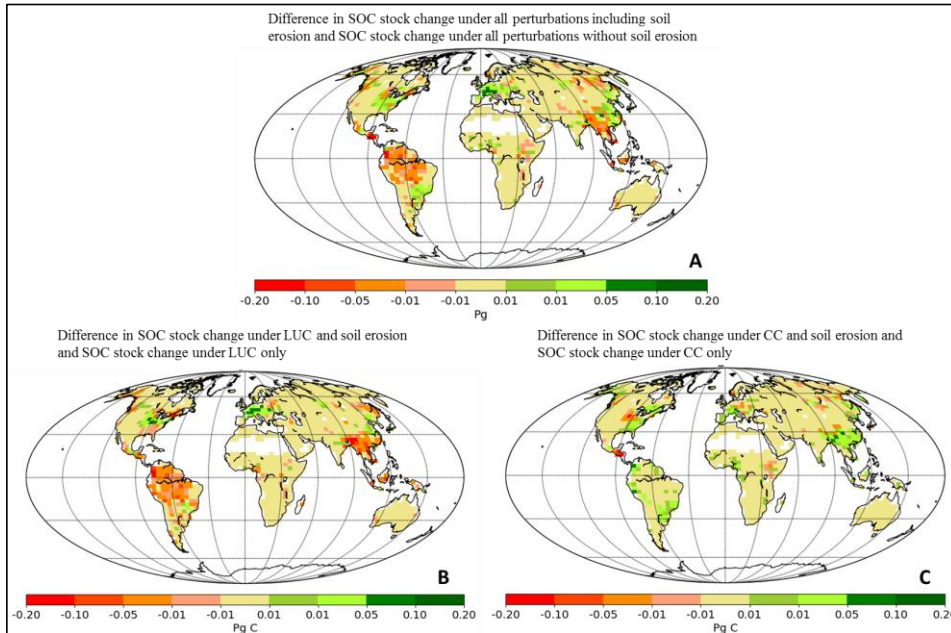


Figure 6: Cumulative SOC stock changes during 1850 – 2005 for (A) simulations with variable atmospheric CO₂ concentration, and (B) for simulations with a constant CO₂ concentration, implied by variable land cover alone (dash-dotted lines), by variable climate (dashed lines), and variable land cover and climate (straight lines), without erosion (black lines) and with erosion (red lines).



987 Figure 7: Cumulative SOC stock changes per PFT during 1850 – 2005 implied by variable land cover, climate and CO₂, without erosion (grey colors) and with erosion (red colors).



994 Figure 8: A) Difference between the changes of SOC stocks over the period 1850-2005 under all perturbations including soil erosion and the changes in SOC stocks excluding soil erosion, S1-S3, B) Difference between the changes of SOC stocks under LUC including soil erosion and the changes in SOC stocks excluding soil erosion (S1-S2)-(S3-S4), C) Difference between the changes of SOC stocks under a variable climate and CO₂ increase including soil erosion and the changes in SOC stocks excluding soil erosion, S2-S4.

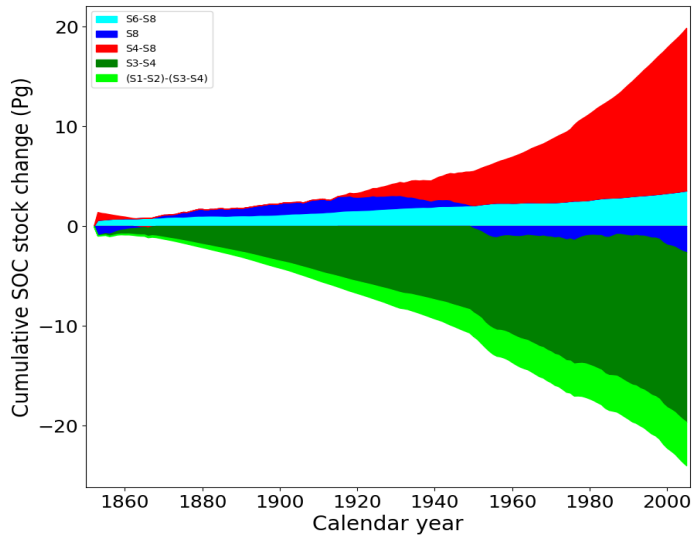


Figure 9: Contribution to the cumulative global SOC stock change over 1850-2005 by CO₂ fertilization (red), effect of precipitation and temperature change on the carbon cycle (dark blue), effect of precipitation change on soil erosion (aqua), LUC effect on the carbon cycle (dark green), and LUC effect on soil erosion (light green)